CONF-800909--1

ON THE ABILITY OF THE TRAC-P1A COMPUTER PROGRAM TO PREDICT BLOWDOWN, REFILL, AND REFLOOD PHENOMENA DURING SEMISCALE MOD-1 EXPERIMENTS

Paul N. Demmie
EG&G Idaho, Inc.
Idaho Falls, Idaho 83415, U.S.A.

ABSTRACT

A computer analysis of a Semiscale Mod-1 Loss-of-Coolant Experiment (LOCE) was performed using the TRAC-P1A computer program. The main purpose of this analysis was to contribute data for the assessment of the ability of TRAC-P1A to predict blowdown, refill, and reflood phenomena during a postulated Loss-of-Coolant Accident (LOCA). A TRAC-P1A Semiscale Mod-1 system model was created and TRAC-P1A was used to obtain initial conditions for Semiscale Mod-1 LOCE S-04-6. After this initialization, TRAC-P1A was used to simulate the first 60 seconds of this experiment. The results of this simulation are presented and discussed.

1. INTRODUCTION

A computer analysis of a Semiscale Mod-1 Loss-of-Coolant Experiment (LOCE) was performed using the TRAC-P1A computer program.[1] The main purpose of this analysis was to contribute data for the assessment of the ability of TRAC-P1A to predict blowdown, refill, and reflood phenomena during a postulated Loss-of-Coolant Accident (LOCA). A second purpose of this analysis was to formulate a set of modeling techniques for application of TRAC-P1A to further analyses of Semiscale Mod-1 experiments.

The Transient Reactor Analysis Code (TRAC) is an advanced best estimate systems computer program designed for the analysis of postulated accidents in light water reactors. TRAC-P1A is an improved version of TRAC-P1, the first publically released version of TRAC which was designed primarily for the analysis of large break LOCAs in pressurized water reactors. The main features of TRAC are a three-dimensional representation of the reactor pressure vessel with two-fluid nonequilibrium fluid dynamic models and a one-dimensional representation of piping and other components with two-phase nonequilibrium fluid dynamic models. Other features include a flow-regime dependent constitutive equation package, comprehensive heat transfer capability, a consistent analysis of entire accident sequences, and component and functional modularity.

The simulation of the first 60 seconds of LOCE S-04-6 was used to evaluate the ability of TRAC-P1A to predict blowdown, refill, and reflood phenomena during Semiscale Mod-1 experiments. This simulation is discussed in Section 2. In this section short descriptions of the Semiscale Mod-1 experimental apparatus and LOCE S-04-6 are given. A description of the TRAC-P1A Semiscale Mod-1 system model used in this simulation is found in Section 2.1. In Section 2.2 some operational information about this simulation is found.

A presentation and discussion of the results of this simulation are given in Section 3. Included in this presentation are plots showing rod cladding temperatures, pressures, mass and volumetric flows, and densities as calculated by TRAC-P1A and as measured during LOCE S-04-6.

The conclusions obtained from this computer analysis of Semiscale Mod-1 LOCE S-04-6 and some recommendations based on these conclusions are given in Section 4.

2. THE SIMULATION OF SEMISCALE MOD-1 LOCE S-04-6

The simulation of the first 60 seconds of Semiscale Mod-1 LOCE S-04-6 was used to evaluate the ability of TRAC-P1A to predict blowdown, refill, and reflood phenomena during Semiscale Mod-1 experiments. A description of the TRAC-P1A Semiscale Mod-1 system model used in this simulation is found in Section 2.1. In Section 2.2 some operational information about this simulation is given.

The Semiscale Mod-1 system[2] is a small scale model of a four-loop pressurized water reactor (PWR). It consists of a pressure vessel with simulated reactor internals (downcomer, lower plenum, core region, and upper plenum); an intact loop with a pressurizer, steam generator, active pump, and associated piping; a broken loop with a simulated steam generator, simulated pump, associated piping, and break assemblies; a pressure suppression system with a header and suppression tank; and a coolant injection system with high and low pressure injector pumps and accumulators. The core region contains 40 electrically heated rods. The heated length of each of these rods is 1.68 m with ten power steps providing a slightly bottom-skewed axial power profile. A radial power peaking factor can be applied to the center four rods.

Semiscale Mod-1 LOCE S-04-6 was the sixth experiment in the baseline emergency core cooling (ECC) test series which was designed to study the integral blowdown-reflood response of the Semiscale Mod-1 system with an electrically heated core.[3] It simulated a complete double-ended offset shear break in a cold leg of a PWR with ECC injection into the intact and broken loop cold legs. Three of the four center rods and 33 of the remaining 36 rods were powered. The remaining, unpowered rods simulated control rods within the reactor core. The fluid conditions prior to blowdown initiation were those conditions obtained by maintaining a volumetric flow through the core and intact loop of 8.895×10^{-3} m^3/s at a system pressure of 1.5528×10^7 N/m^2 with a core power of 1.44 MW. After blowdown initiation the electrical power in the powered rods was programmed in such a manner that the thermal response of each rod simulated the thermal response of a nuclear rod.

2.1 TRAC-P1A Semiscale Mod-1 System Model

The TRAC-P1A Semiscale Mod-1 system model used for this simulation of LOCE S-04-6 was formulated after an extensive study of the Semiscale Mod-1 system. The choices made in selecting components and options in this model were based on an attempt to accurately represent the Semiscale Mod-1 system with TRAC-P1A's capabilities as ascertained from Reference 1 and user experience at the Idaho National Engineering Laboratory. The main features of this model are:

1. The vessel contains 18 axial levels with each axial level containing two radial segments and two azimuthal segments. This nodalization has 72 cells in the vessel. The lower plenum is represented by two of these axial levels, and the upper plenum is represented by one of these axial levels.

2. The active heated rods are represented axially with 10 of the 18 vessel axial levels. Each rod level corresponds to a power step in the slightly bottom-skewed axial power profile. Each heated rod has 10 radial heat transfer nodes.

3. Each cell in the vessel has a lumped parameter heat slab whose area and mass are determined from the actual area and volume of vessel material thermally interacting with it.

4. The intact loop is represented by two tee components, a steam generator component, a pipe component, and a pump component. A pressurizer is connected to the secondary of one tee component, and intact loop ECC piping is connected to the secondary of the other tee component. Feedwater flow in the steam generator secondary is maintained for the required one second using a fill component with the velocity versus time option. A break component with the constant pressure option is connected to the other end of the steam generator secondary.

5. The pump speed versus time option was used in the pump component since the pump coastdown option was found to produce a considerably retarded coastdown rate.

6. The broken loop is represented by a pipe and a tee component. The piping represented by these components includes the simulated steam generator and pump, the break nozzles, and piping from the break nozzles to the pressure suppression system. The broken loop ECC piping is connected to the secondary of the tee component.

7. The pressure suppression system is represented by break components with the constant pressure option. These components are connected to the broken loop pipe and tee components.

8. The break nozzles are finely nodalized to attempt to calculate break flow correctly.

9. The intact and broken loop ECC systems each are represented by an accumulator component, a valve component with the check valve option, two fill components representing the high pressure injection system (HPIS) and the low pressure injection system (LPIS) pumps, and two tee components. The fill components employ the velocity versus pressure option to simulate actual pump performance.

10. The fully-implicit hydrodynamics option is employed exclusively in the components connected to the vessel. This option is particularly important in the broken loop where the cell lengths are quite varied.

11. In all one-dimensional components representing piping or pumps, wall heat transfer with one heat transfer node is calculated. The thermal coupling between the steam generator's primary and secondary is accomplished using three heat transfer nodes. Critical heat flux calculations are performed only in the vessel and the steam generator secondary.

12. The homogeneous flow friction factor was used in all components where a choice is required. Added friction was included as calculated for area change losses, bends, tees, and instrumentation. Added friction was also included as experimentally determined for the pressurizer surge line, the accumulator lines, the steam generator, the simulated steam generator and pump, and the core to upper plenum region.

This Semiscale Mod-1 system model consists of 25 components with 212 computational cells.

This model was modified slightly to obtain the initial conditions for the simulation of LOCE S-04-6. The break components representing the pressure suppression system were replaced with fill components having a zero fill velocity specified for the initialization.

2.2 Discussion of the Simulation

After initial conditions were obtained for the simulation of LOCE S-04-6 by running TRAC-P1A in the steady-state mode for 60 s, the simulation of the first 60 s of LOCE S-04-6 commenced. This simulation required a total of 6.2801 hr central processing unit (CPU) time on the CDC 176 computer - 3.0594 hr for the first 40 s and 3.2217 hr for the last 20 s. The time step sizes were determined internally by TRAC-P1A with a minimum time step size of 1.0×10^{-9} s input and a maximum time step size of 1.0×10^{-2} s input for the first 30 s of the transient and 5.0×10^{-3} s input for the last 30 s. This minimum time step size and the increase in outer iteration number to 100 and outer iteration convergence criterion to 1.0×10^{-2} after 30 s solved the outer iteration convergence problems that occurred after 30 s. All other iteration numbers and convergence criteria were input as recommended in the TRAC-P1A manual.[1]

3. PRESENTATION AND DISCUSSION OF THE RESULTS OF THE SIMULATION OF SEMISCALE MOD-1 LOCE S-04-6

Comparisons of quantities calculated by TRAC-P1A during this simulation of Semiscale Mod-1 LOCE S-04-6 and obtained from the experimental data for this experiment are given in Figures 1 through 23. In these figures time after blowdown initiation is measured along the horizontal axis, and the quantities compared are measured along the vertical axis. In all these figures the unmarked curves are TRAC-P1A calculated quantities, and the curves marked with solid circles are the corresponding quantities obtained from the experimental data.

Since the performance of the heated rods during a postulated LOCA is the primary concern in the analysis of this accident, Figures 1, 2, and 3 show heated rod cladding temperature histories at Power Steps 2, 5, and 8, respectively. These power steps are three of the 10 power steps in the heated core and are located in its lower, middle, and upper parts, respectively. In these figures the unmarked curves are the average calculated temperatures at a given power step. The curves marked with the 1's and the 2's are the low and high extrema, respectively, of the measured temperature data range for the power step depicted, and the curves marked with the stars see the average measured cladding temperatures at the corresponding power step. The data ranges are large, since critical heat flux (CHF), indicated in these figures by a large rate of change of temperature with respect to time, occurs at different times at various thermocouples in a given power step.

Figure 1 shows that the calculated and average measured cladding temperatures agree well at Power Step 2.

Figure 2 shows that the calculated and average measured temperatures do not agree well at Power Step 5, but that the calculated temperatures are within the data range at this high power step during most of the simulation. Actually the peak cladding temperature is predicted within 75 K, although the time at which this peak temperature occurs differs from the time it occurs in the experiment.

Although adequate cladding temperature predictions are made at the lower and high-powered parts of the heated core, the calculated cladding temperatures at Power Step 8 are considerably higher than the data, as shown in Figure 3. The reason for this disagreement is that in LOCE S-04-6 CHF occurs at between 0.5 and 1 s at the lower and middle parts of the heated core and after 2 s at the upper part; whereas TRAC-P1A calculates CHF to occur at approximately 1 s at all these parts. Thus TRAC-P1A's ability to predict heater rod cladding temperatures correlates well with TRAC-P1A's ability to predict the occurrence of CHF.

TRAC-P1A calculates simultaneous CHF without rewet at the lower and upper parts of the heated core. This prediction is seen in Figure 24, which shows the calculated temperatures at Power Steps 2 and 8 for the first 2 s of the simulation. This prediction is consistent with the identical heated rod power and nearly identical fluid conditions at these levels at the time CHF occurs.

Calculated and experimental mass flow histories at the core inlet are shown in Figure 4. This figure shows particularly poor disagreement between calculated and experimental mass flows at approximately 1 s and 56 s. The disagreement early in the simulation is more clearly seen in Figure 25, which shows these mass flow histories during the first 2 s of the simulation.

Figures 5, 6, 7, and 8 show calculated and experimental mass flow histories in the broken loop hot leg, broken loop cold leg, intact loop hot leg, and intact loop cold leg, respectively. In general the calculated and experimental mass flows shown in these figures do not agree well.

The incorrect calculation of mass flows in the broken loop early in the blowdown contributes to the poor calculation of heated rod cladding temperatures at the upper part of the heated core. Figures 5 and 6 show that early in the blowdown the calculated mass flow is too high in the broken loop hot leg and too low in the broken loop cold leg, and Figure 25 shows that the calculated mass flow is incorrect at the core inlet. A better calculation of break mass flow would result in a better calculation of mass flow at the core inlet and more liquid from the upper plenum reaching the upper part of the heated core. More liquid in the upper part of the heated core would delay the initiation of CHF and thus result in a better prediction of cladding temperatures. The additional liquid should improve slightly the prediction of cladding temperatures at the middle part of the heated core, but hardly affect the prediction of cladding temperature at the lower part of the heated core, since this liquid must be reheated in passing from the upper plenum to the lower part of the heated core.

Figures 9, 10, 11, and 12 show calculated and measured pressure histories in the upper plenum, pressurizer, intact loop accumulator, and broken loop accumulator, respectively. Except for between approximately 34 and 54 s the calculated system (upper plenum) pressure does not agree well with this measured system pressure. This disagreement results primarily from the poor break mass flow calculation. Although this calculation contributes to the disagreement between calculated and measured pressures in the pressurizer and accumulators, the use of added friction, obtained from experimentally determined hydraulic resistances in the pressurizer and accumulator lines, resulted in excessive friction in these lines. The exclusion of this added friction and an improvement in the break flow calculation would result in a significant improvement in calculated pressures.

Figures 13, 14, 15, 16, and 17 show calculated and experimental densities at the core inlet, in the broken loop hot leg, broken loop cold leg, intact loop hot leg, and intact loop cold leg. These figures show that in general the calculated and experimental densities do not agree well.

In Figure 13 a significant disagreement in densities at the core inlet is seen after 55 s. Since refill occurs in LOCE S-04-6 at approximately 55 s, this disagreement indicates that refill has not occurred during this simulation of LOCE S-04-6. Figure 26, which gives the liquid volume fraction of the lower plenum, shows that the lower plenum has not even refilled during this simulation.

Poor intact loop ECC performance during the simulation could be responsible for the failure of the lower plenum to refill. Figures 18 through 23 show the performance of the ECC system during this simulation. These figures give the respective calculated and measured volumetric flows in the intact loop accumulator, intact loop HPIS pump, intact loop LPIS pump, broken loop accumulator, broken loop HPIS pump, and broken loop LPIS pump. Outstanding features of these figures are that during the simulation intact loop accumulator flow was initiated about 4 s early, broken loop accumulator flow was initiated about 9 s late, and the intact loop LPIS flow was zero for most of the simulation. The agreement between the calculated and measured volumetric flows shown in these figures would be better if the agreement between calculated and measured pressures were better.

The low intact loop LPIS flow suggests that an explanation for the failure of the lower plenum to refill is that not enough intact loop ECC liquid was injected into the vessel. However, Figure 27 shows that sufficient intact loop ECC liquid was injected into the vessel. Figure 27 gives the total calculated and measured intact loop accumulator, HPIS, and LPIS volumetric flows. This figure shows that the amount of ECC liquid injected during this simulation of LOCE S-04-6 is larger than the amount of ECC liquid injected during LOCE S-04-6.

The reason that refill failed to occur during this simulation is not that insufficient liquid was injected by the ECC system, but that only one-sided, lumped-parameter heat slabs are available to model heat transfer between the fluid in the downcomer and lower plenum and the downcomer and lower plenum walls. Since the heat slabs are one-sided, the only mechanisms available for cooling the heat slabs representing the downcomer and lower plenum walls are the vaporization of ECC liquid and the superheating of the resulting steam. Therefore, refill is delayed because these heat slabs cannot also be cooled by energy transfer to the atmosphere or core region. Furthermore, the uniform temperature heat slab assumption implicit in the lumped-parameter heat transfer solution technique is not valid for heat slabs of the masses used in this Semiscale Mod-1 system model and results in overestimating the rate at which energy is transferred to the fluid. Refill is also delayed considerably by this higher than realistic energy transfer rate.

4. CONCLUSIONS AND RECOMMENDATIONS

Since the performance of the heated rods during a postulated LOCA is the primary concern in the analysis of this postulated accident, the main conclusion of this analysis is:

1. An adequate prediction of heated rod cladding temperatures during the blowdown and refill phases of Semiscale Mod-1 LOCE S-04-6 is provided by TRAC-P1A where it correctly predicts the occurrence of CHF.

During this simulation of LOCE S-04-6 the calculated heated rod cladding temperatures agree well with experimental data in the lower part of the heated core and fall within the data in the high-powered part of the heated core, where CHF occurs in LOCE S-04-6 between 0.5 and 1 s. However, in the upper part of the heated core, where CHF occurs in LOCE S-04-6 after 2 s, the calculated heated rod cladding temperatures are considerably higher than the experimental data. At all these core levels TRAC-P1A predicts CHF to occur at approximately 1 s. Thus TRAC-P1A's ability to predict heated rod cladding temperatures correlates well with TRAC-P1A's ability to predict the occurrence of CHF.

It is concluded from the comparisons in Section 3 of quantities calculated by TRAC-P1A during this simulation of LOCE S-04-6 and quantities obtained from the experimental data that:

2. The mass flows, pressures, and densities calculated by TRAC-P1A during this simulation of LOCE S-04-6 do not in general agree well with these quantities obtained from the experimental data.

This conclusion has significance for the poor calculation of heated rod cladding temperature at the upper part of the heated core, since the simultaneous prediction of the occurrence of CHF without rewet at the lower and upper parts of the Semiscale Mod-1 heated core is consistent with the identical heated rod power and nearly identical fluid conditions at these levels at the time this CHF occurs. Based on this conclusion, in particular as it applies to the broken loop mass flows during the blowdown phase of LOCE S-04-6, and the importance of calculating the correct break mass flow for calculating the correct system behavior during a LOCE, it is recommended that:

3. A critical flow model should be developed and implemented in TRAC-P1A to better predict blowdown phenomena during a LOCE or postulated LOCA.

Clearly the results of this simulation show that break flow was poorly calculated although the break nozzles were finely nodalized. Critical flow modeling must be implemented in TRAC-P1A to better calculate break flow. This modeling would lead to a better prediction of system behavior during a LOCE or postulated LOCA.

From the results and discussion presented in Section 3 pertaining to the refill phase of this simulation of LOCE S-04-6, it is concluded that:

4. Refill of the lower plenum did not occur during this 60 s simulation of Semiscale Mod-1 LOCE S-04-6, although refill did occur in LOCE S-04-6 at approximately 55 s. A significant factor in causing this refill delay is the use of one-sided, lumped-parameter heat slabs in the TRAC-P1A vessel component.

Although sufficient ECC liquid was injected into the vessel to refill the lower plenum, the only mechanisms available for cooling the heat slabs representing the downcomer and lower plenum walls are the vaporization of this ECC liquid and the superheating of the resulting steam, since the heat slabs are one-sided and hence thermally interact only with the fluid in the downcomer and lower plenum. Therefore, refill of the lower plenum would occur sooner if the heat slabs were two-sided and thus would also permit cooling the heat slabs by energy transfer to the atmosphere or core region. Furthermore, the uniform temperature heat slab assumption implicit in the lumped-parameter heat transfer solution technique is not valid for heat slabs of the masses used in this Semiscale Mod-1 system model and results in overestimating the rate at which energy is transferred to the fluid. This higher than realistic energy transfer rate also contributes considerably to delaying refill. Therefore, it is recommended that:

5. Although reducing the heat slab masses used in a Semiscale Mod-1 system model by assuming some "effective thickness" would lead to a better prediction of refill phenomena during a LOCE, two-sided heat slabs should be implemented in the TRAC-P1A vessel component and a distributed-parameter heat transfer solution technique should be employed in determining the temperature evolution of these heat slabs.

Such two-sided, distributed-parameter heat slabs are employed in the TRAC-P1A one-dimensional piping components and should also be employed in the TRAC-P1A vessel component. If this recommendation and the recommendation given in Item 3 were followed, then the ability of TRAC-P1A to predict blowdown, refill, and reflood phenomena during Semiscale Mod-1 experiments would be enhanced.

5. REFERENCES

1. Liles et at, TRAC-P1A An Advanced Best-Estimate Computer Program for PWR LOCA Analysis, Vol. 1, NUREG/CR-0665, LA-7777-MS, May 1979.

2. Ball et al, Semiscale Program Description, TREE-NUREG-1210, May 1978.

3. Crapo et al, Experimental Data Report for Semiscale Mod-1 Tests S-04-5 and S-04-6 (Baseline ECC Tests), TREE-NUREG-1045, January 1977.

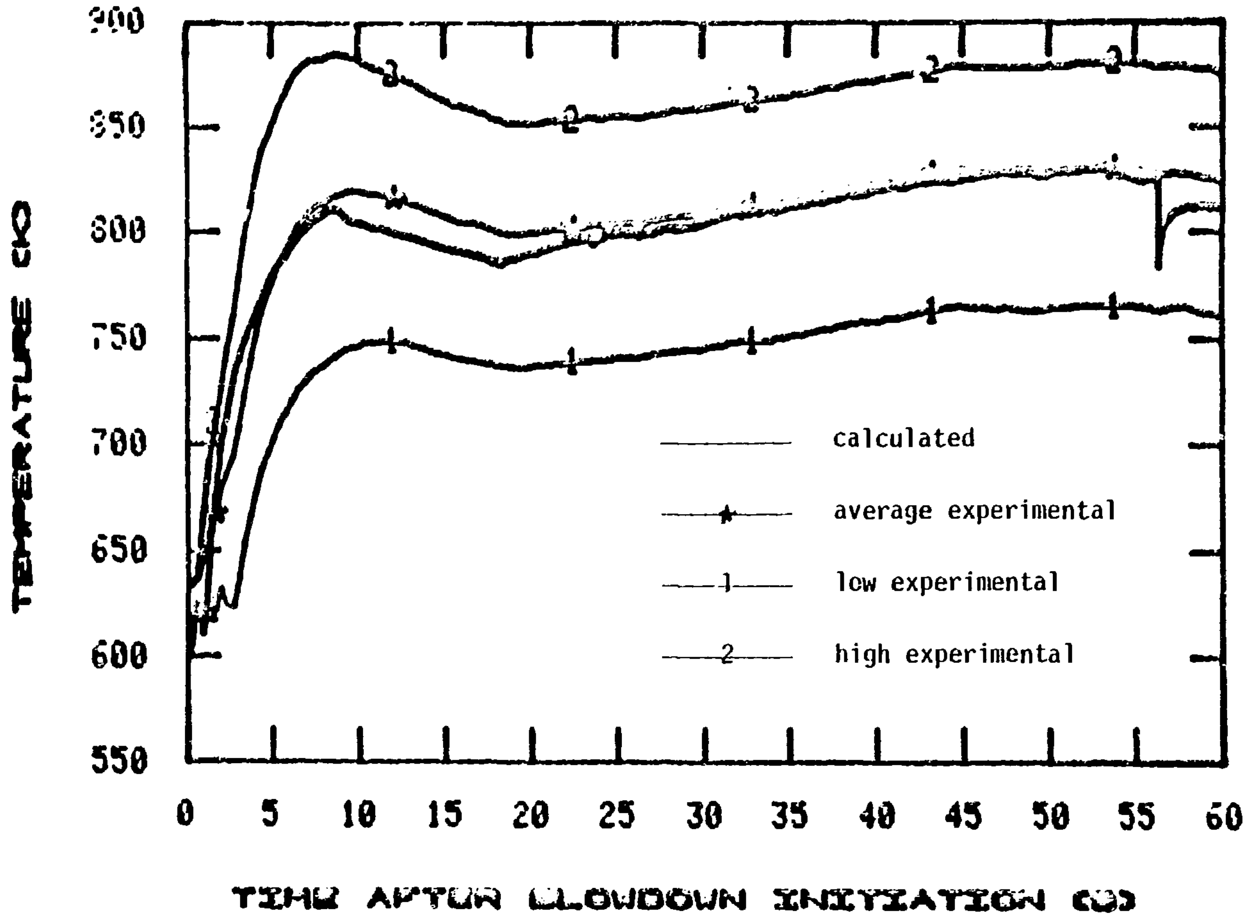

Figure 1 Heated Rod Cladding Temperatures at Power Step 2

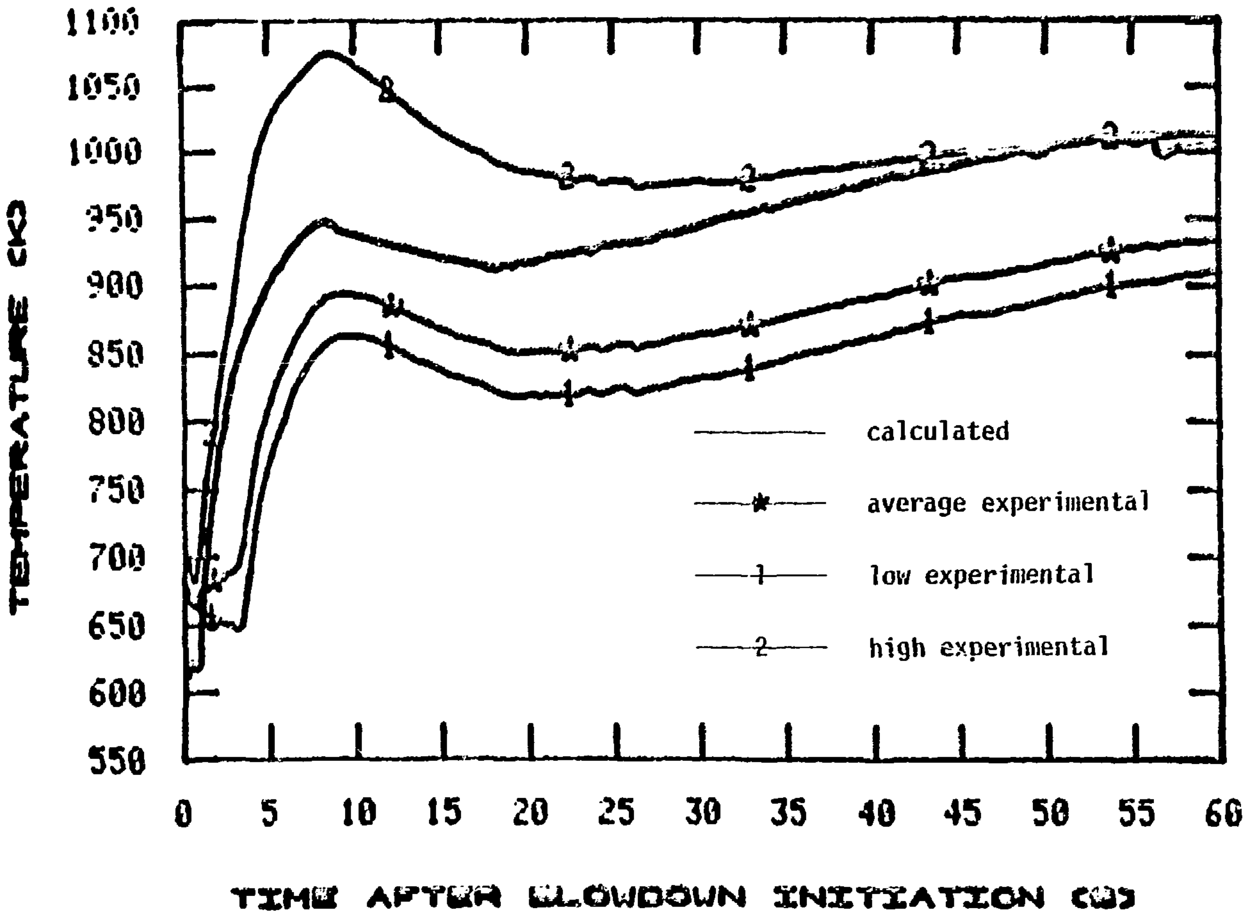

Figure 2 Heated Rod Cladding Temperatures at Power Step 5

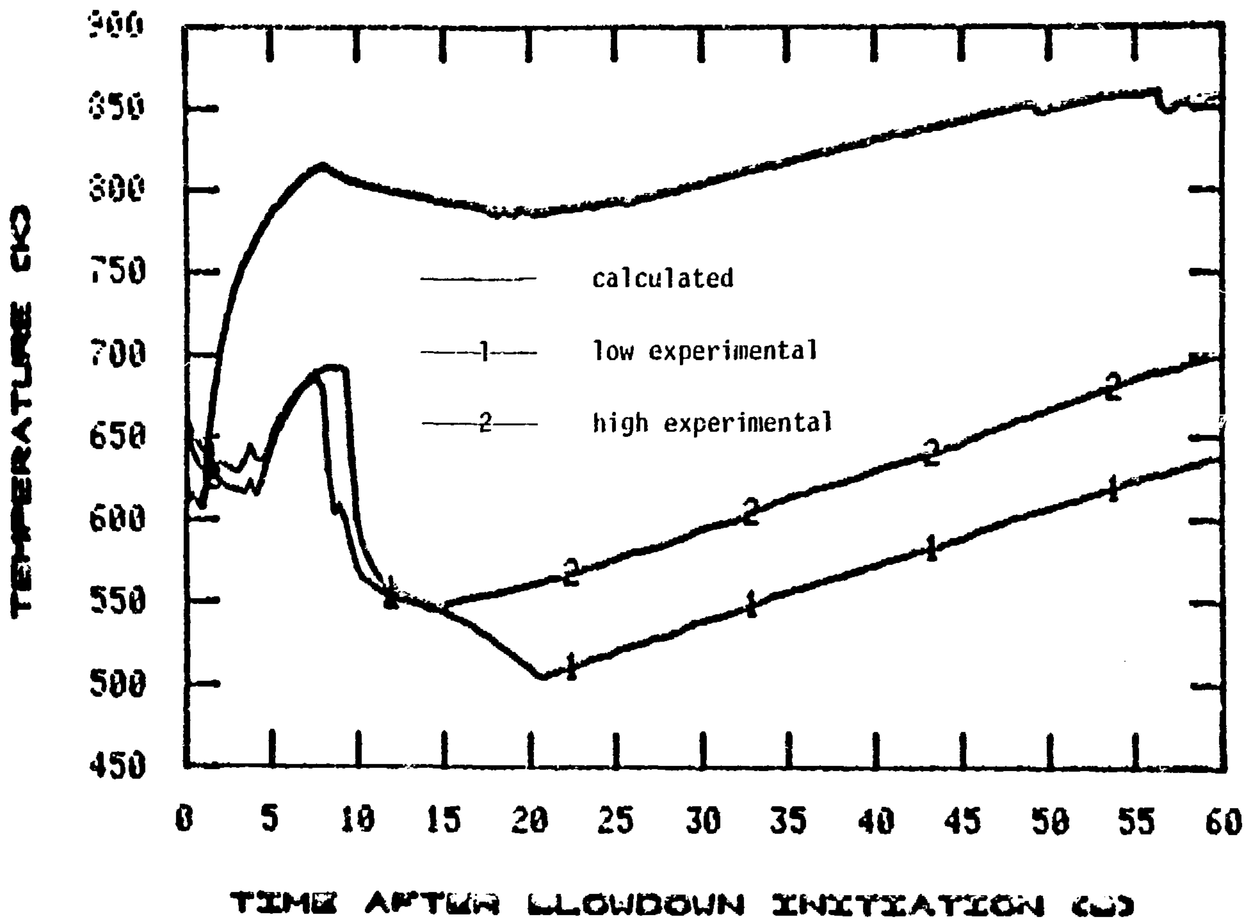

Figure 3 Heated Rod Cladding Temperatures at Power Step 8

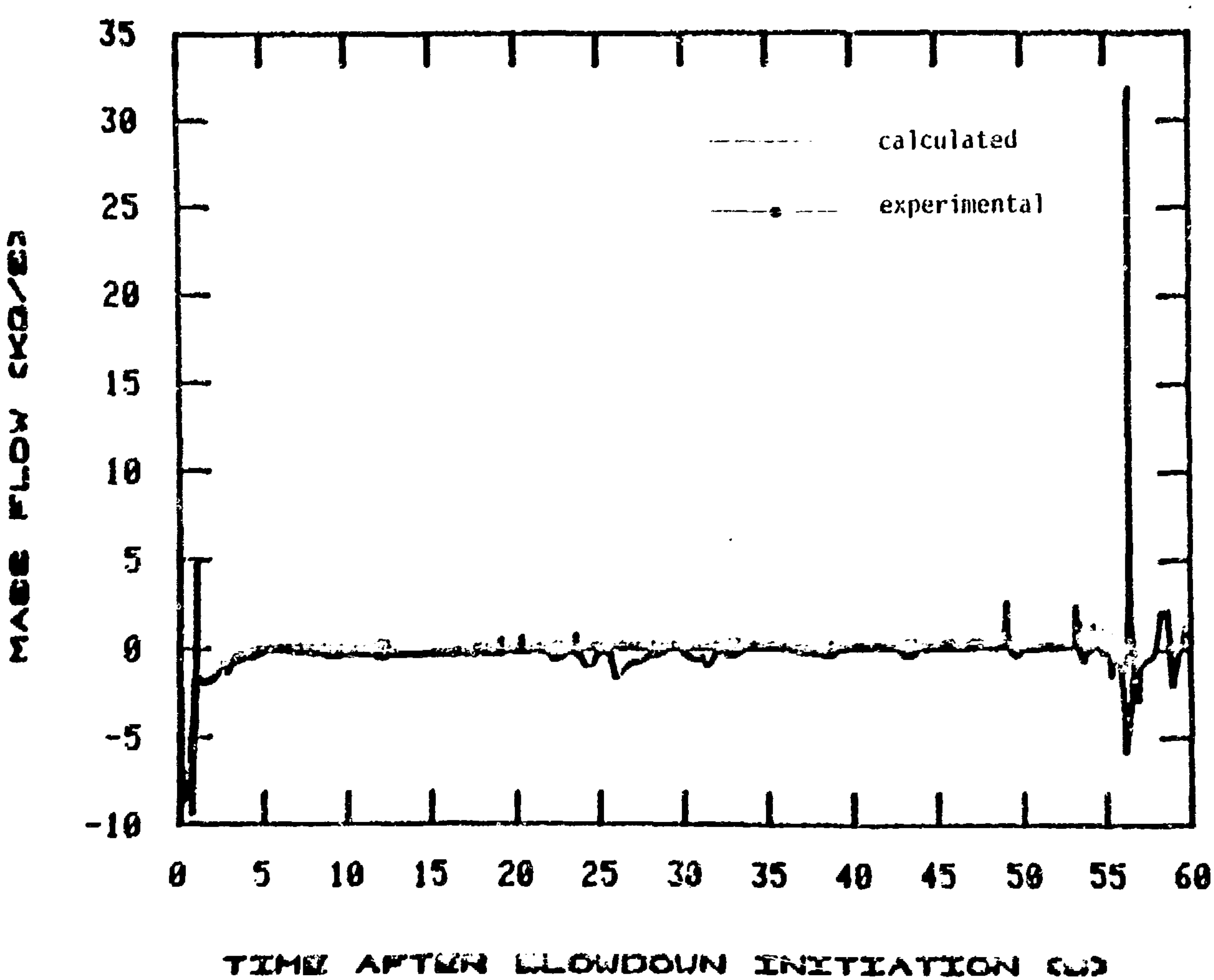

Figure 4 Mass Flows at Core Inlet

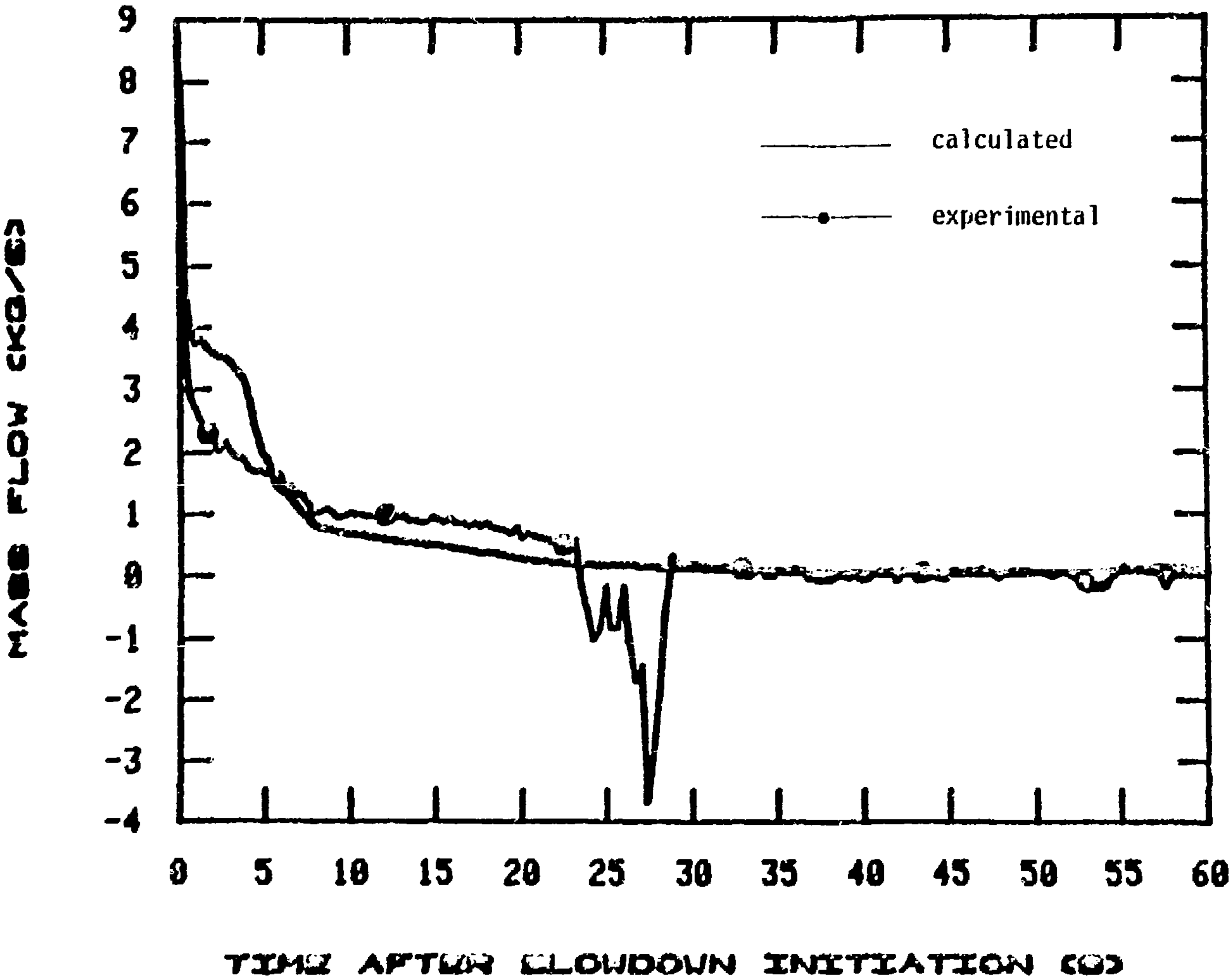

Figure 5 Mass Flows in Broken Loop Hot Leg

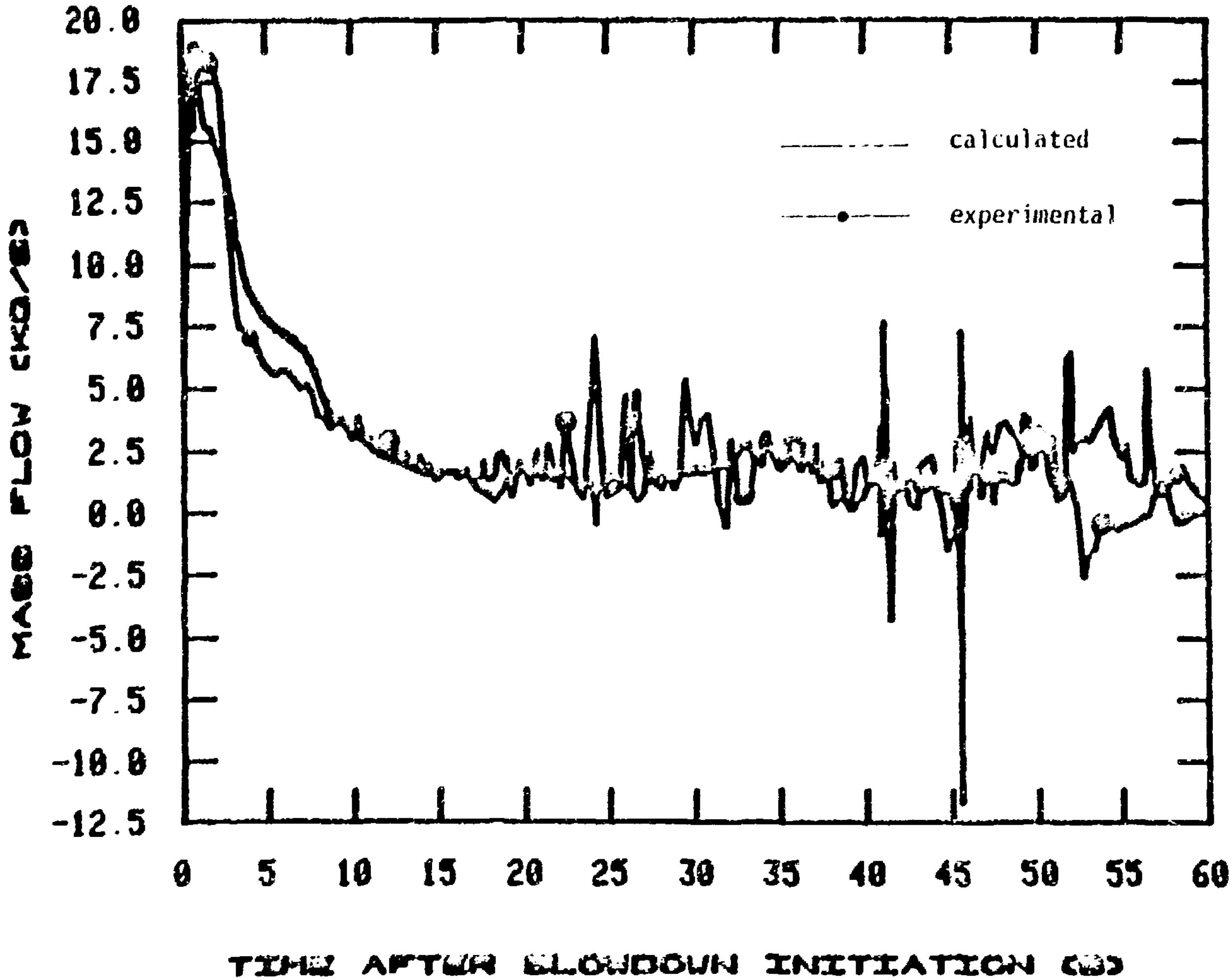

Figure 6 Mass Flows in Broken Loop Cold Leg

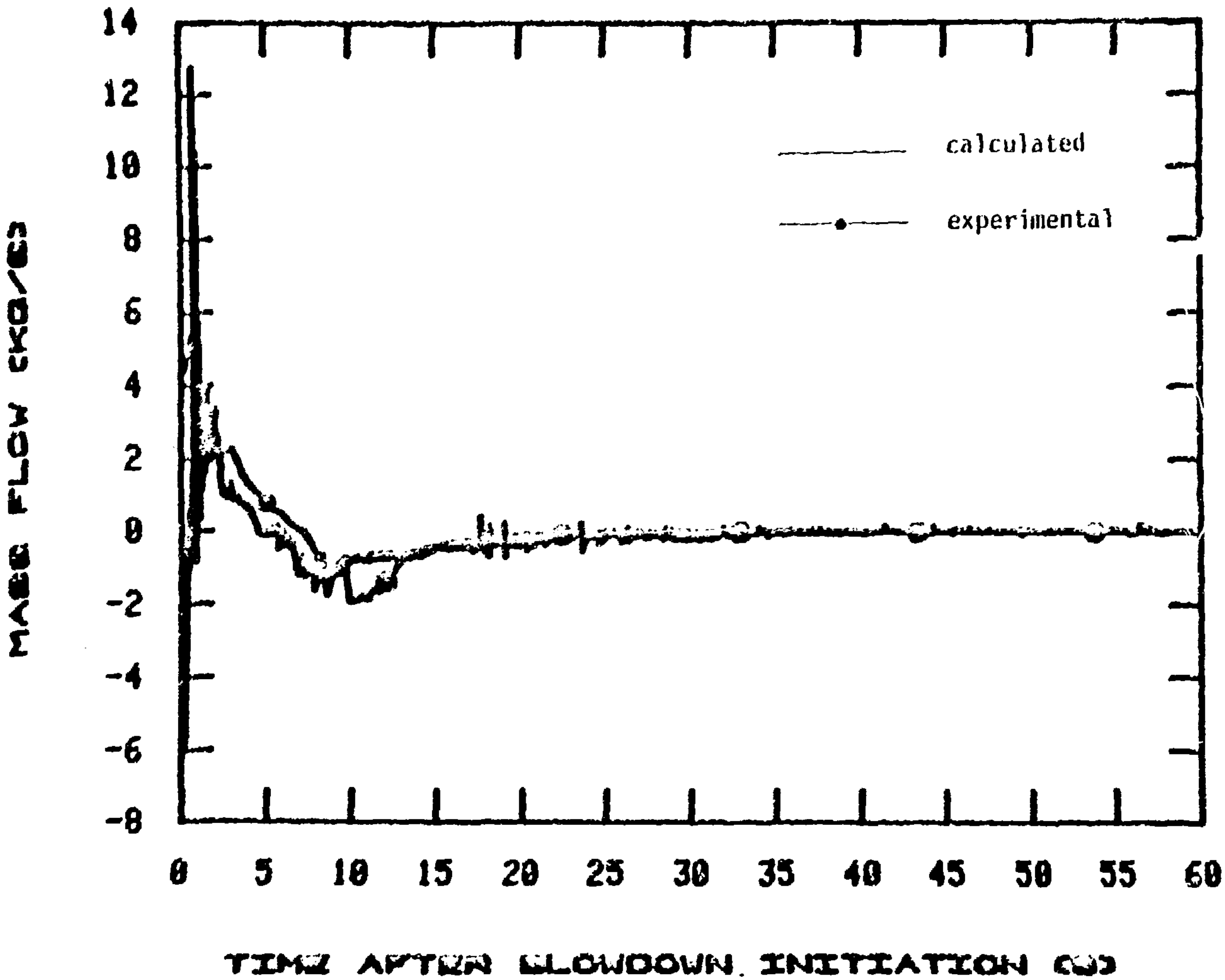

Figure 7 Mass Flows in Intact Loop Hot Leg

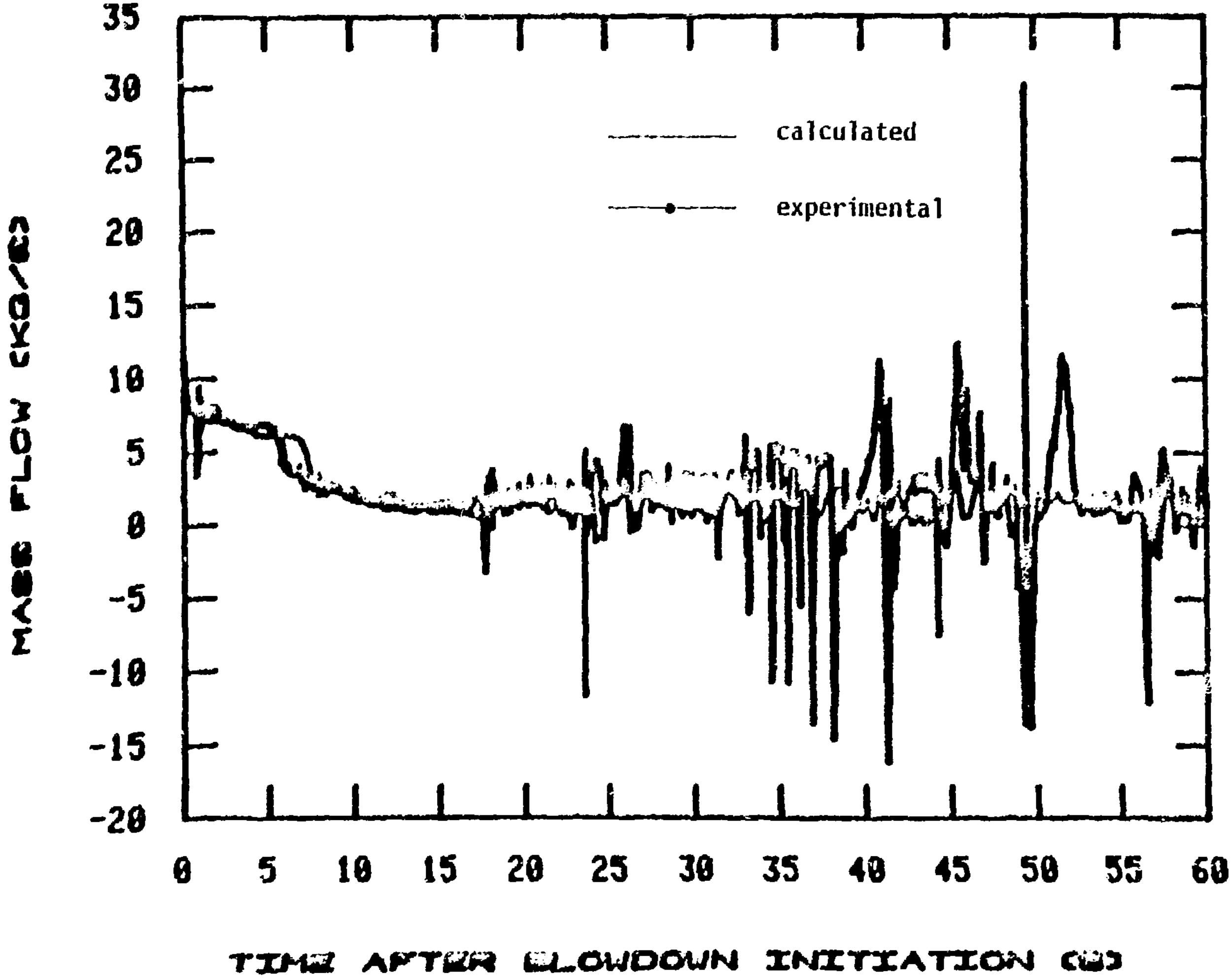

Figure 8 Mass Flows in Intact Loop Cold Leg

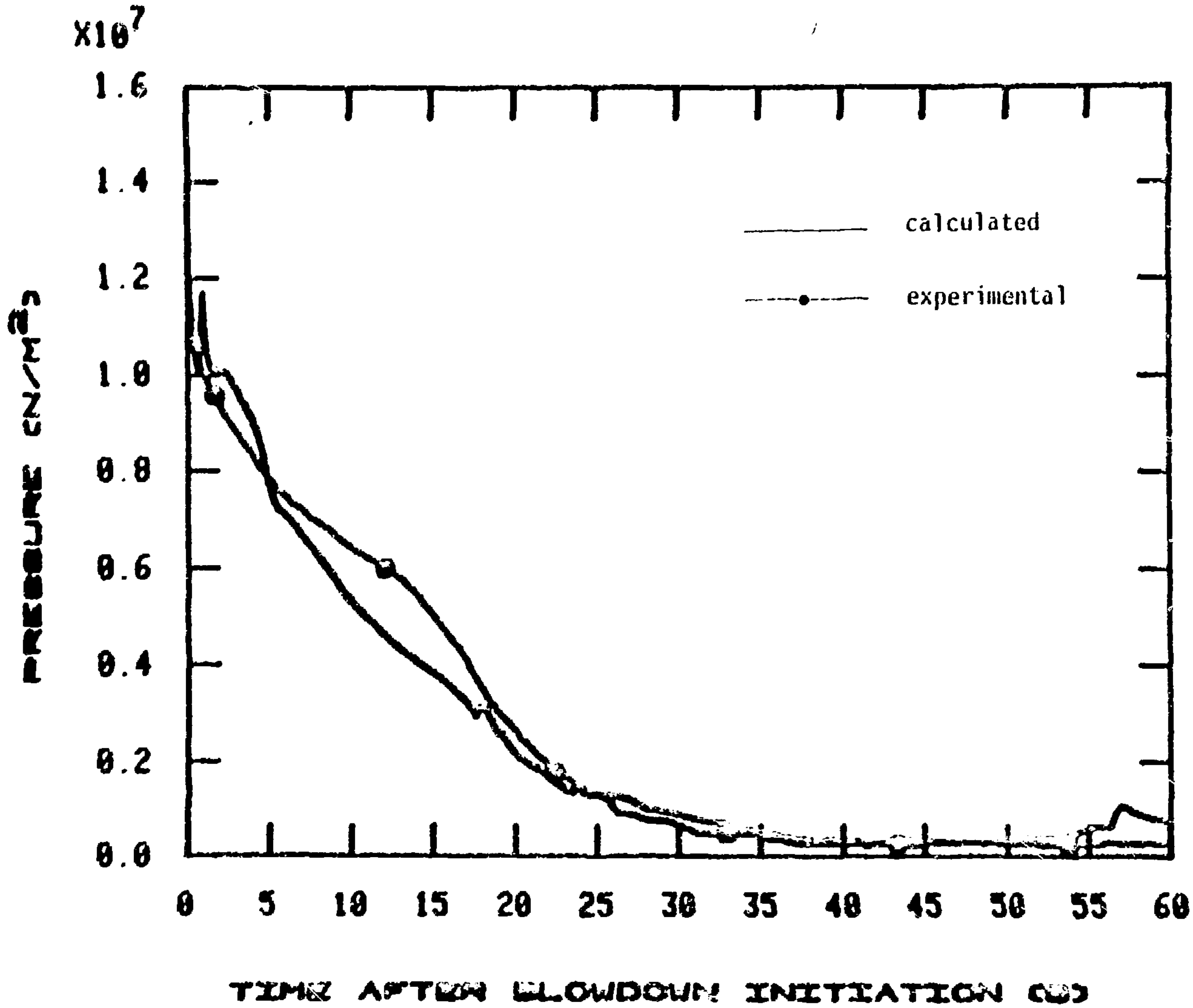

Figure 9 System Pressures

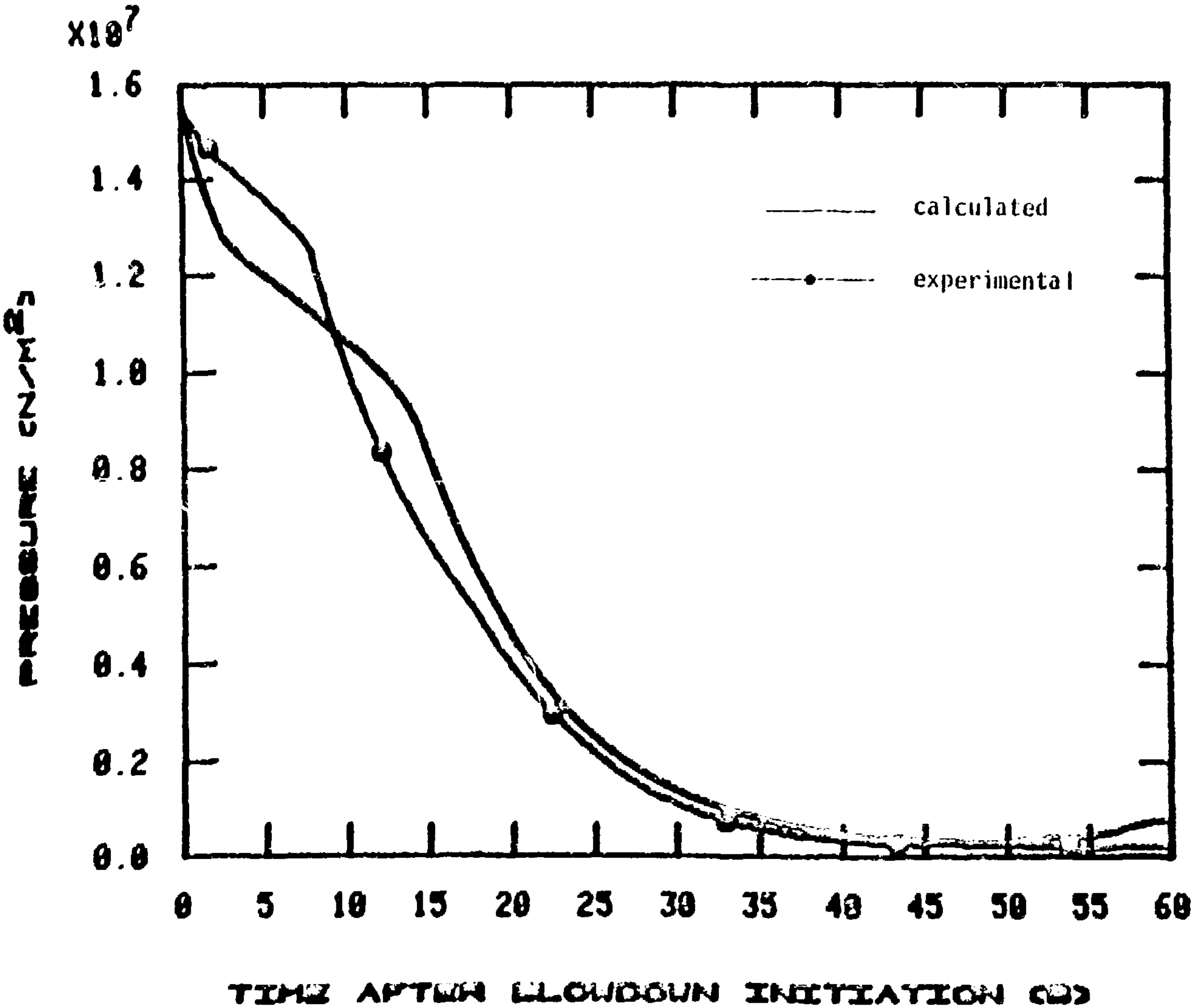

Figure 10 Pressures in Pressurizer

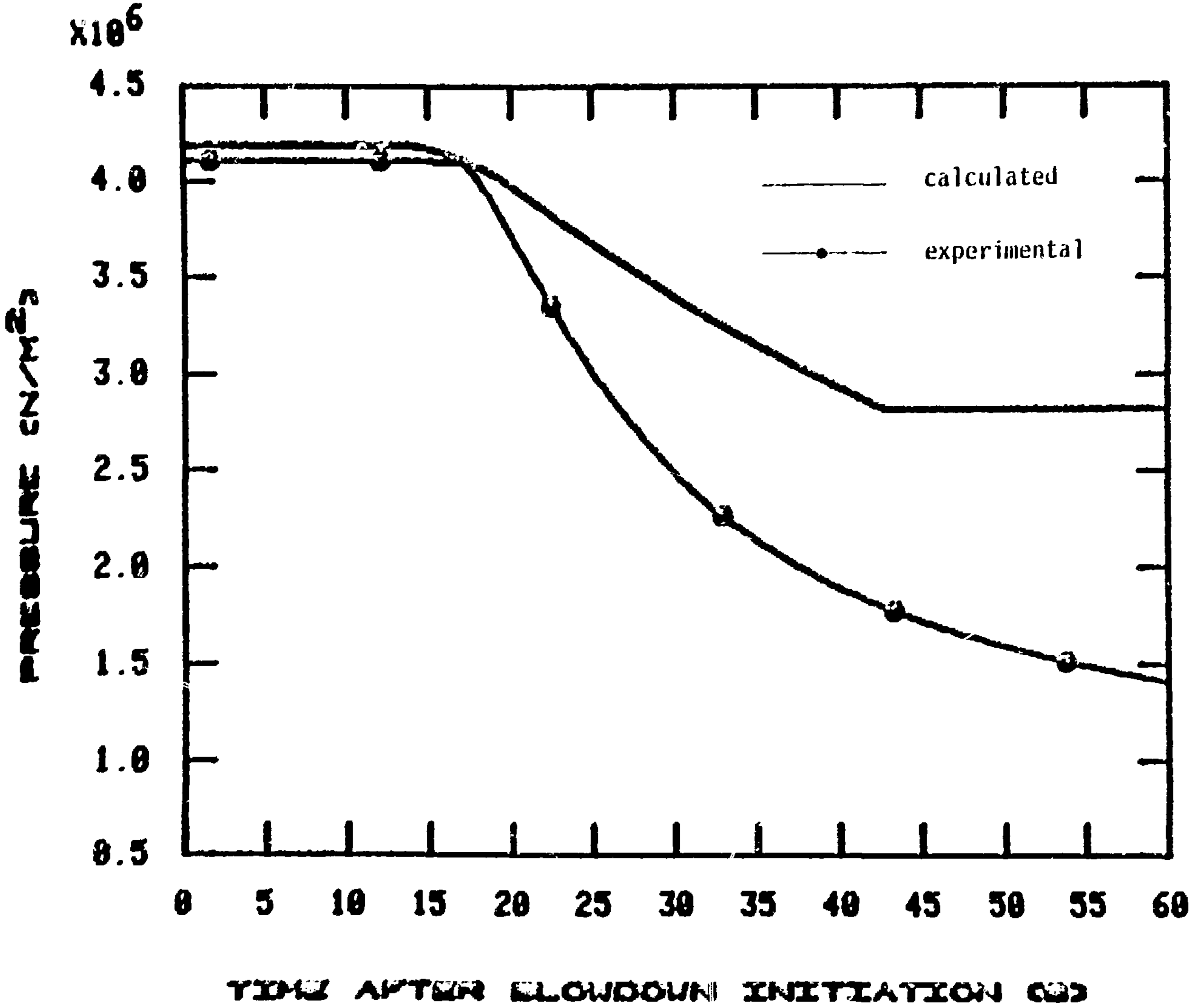

Figure 11 Pressures in Intact Loop Accumulator

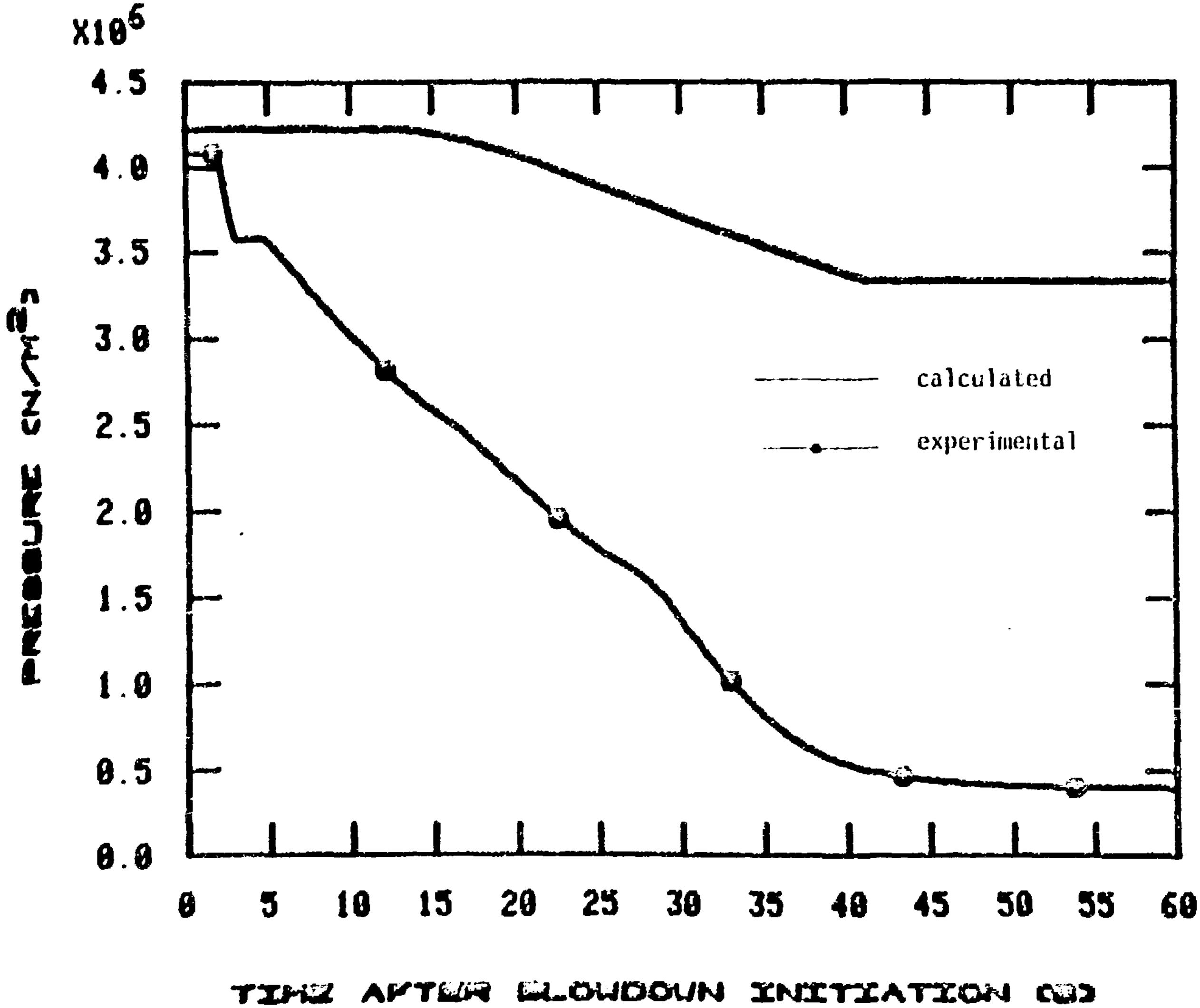

Figure 12 Pressures in Broken Loop Accumulator

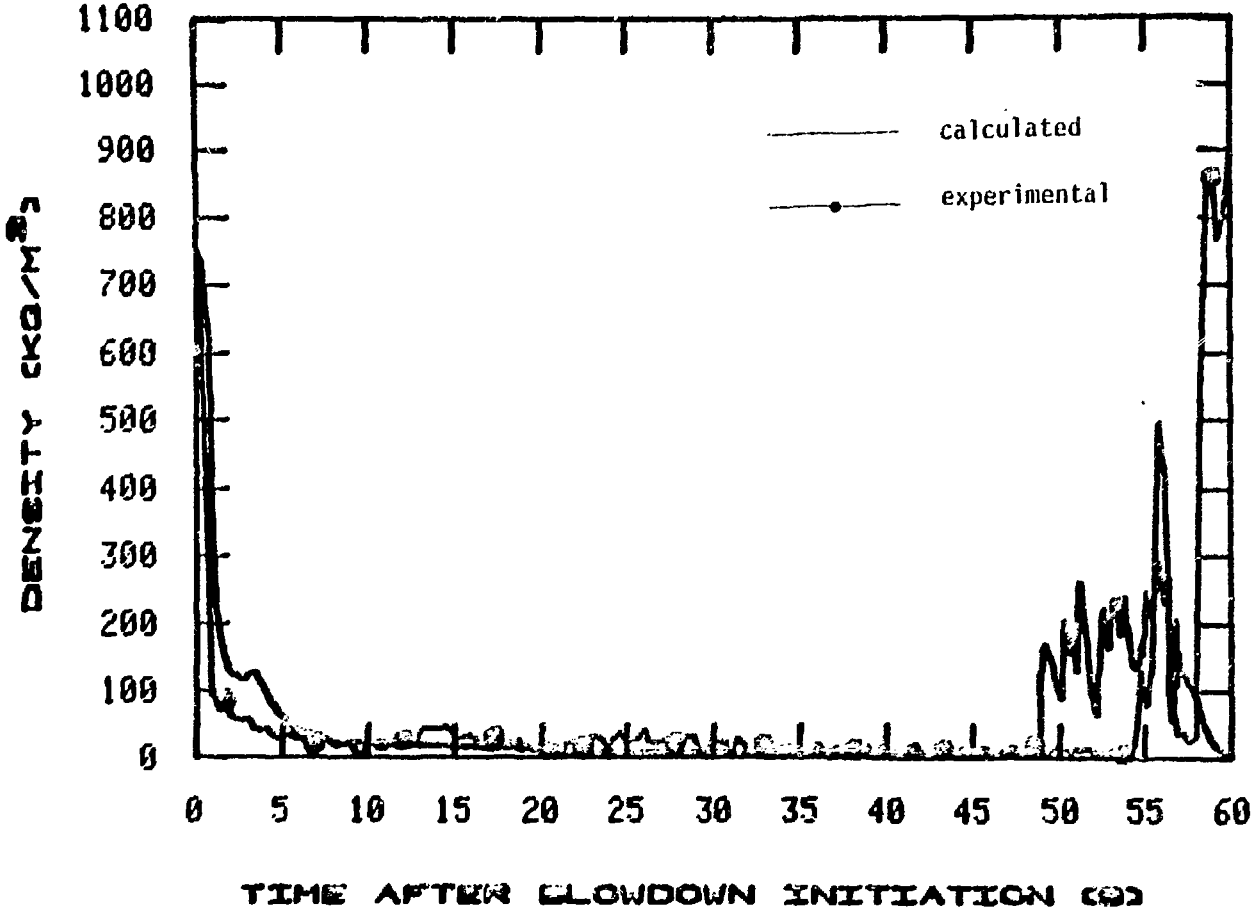

Figure 13 Densities in Core Inlet

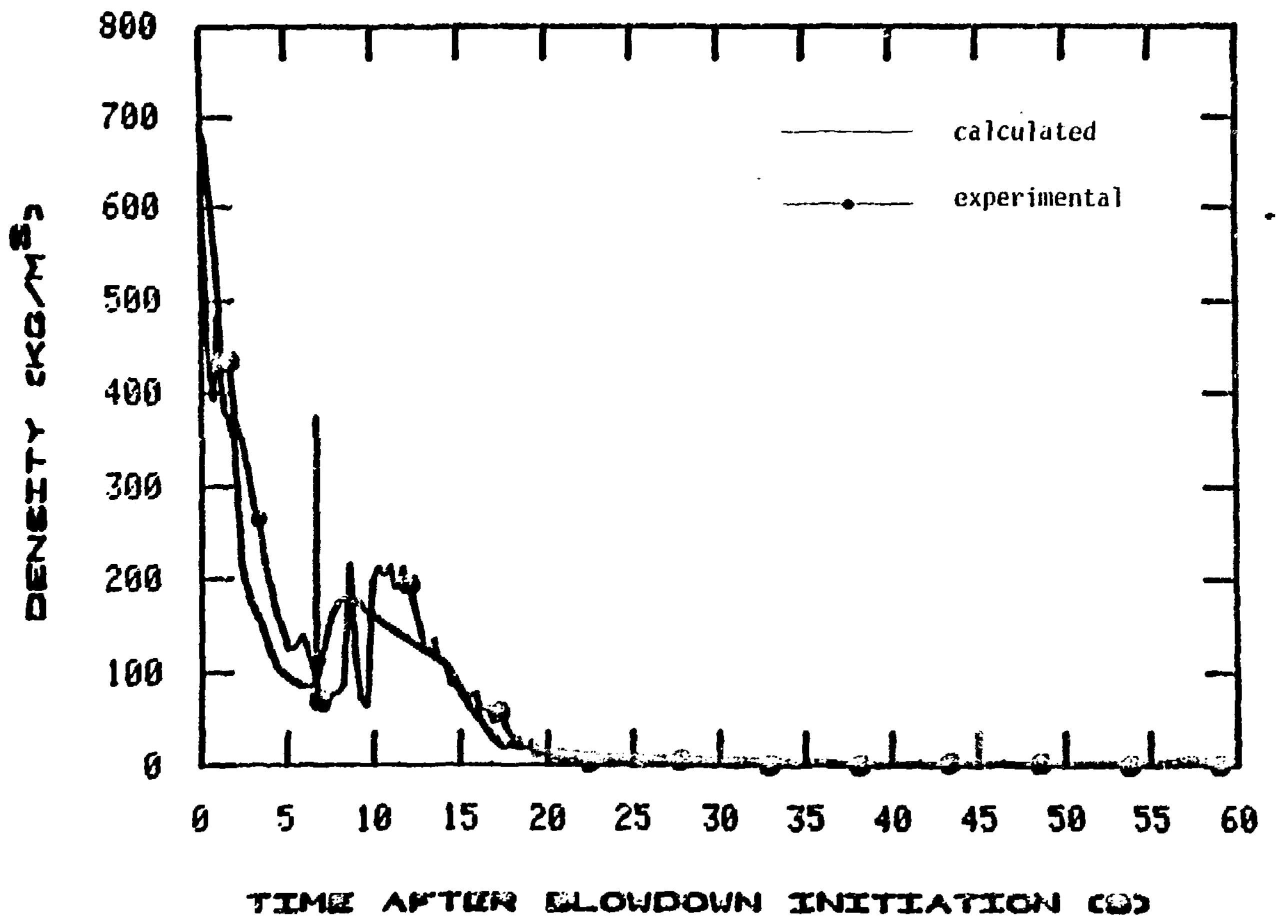

Figure 14 Densities in Broken Loop Hot Leg

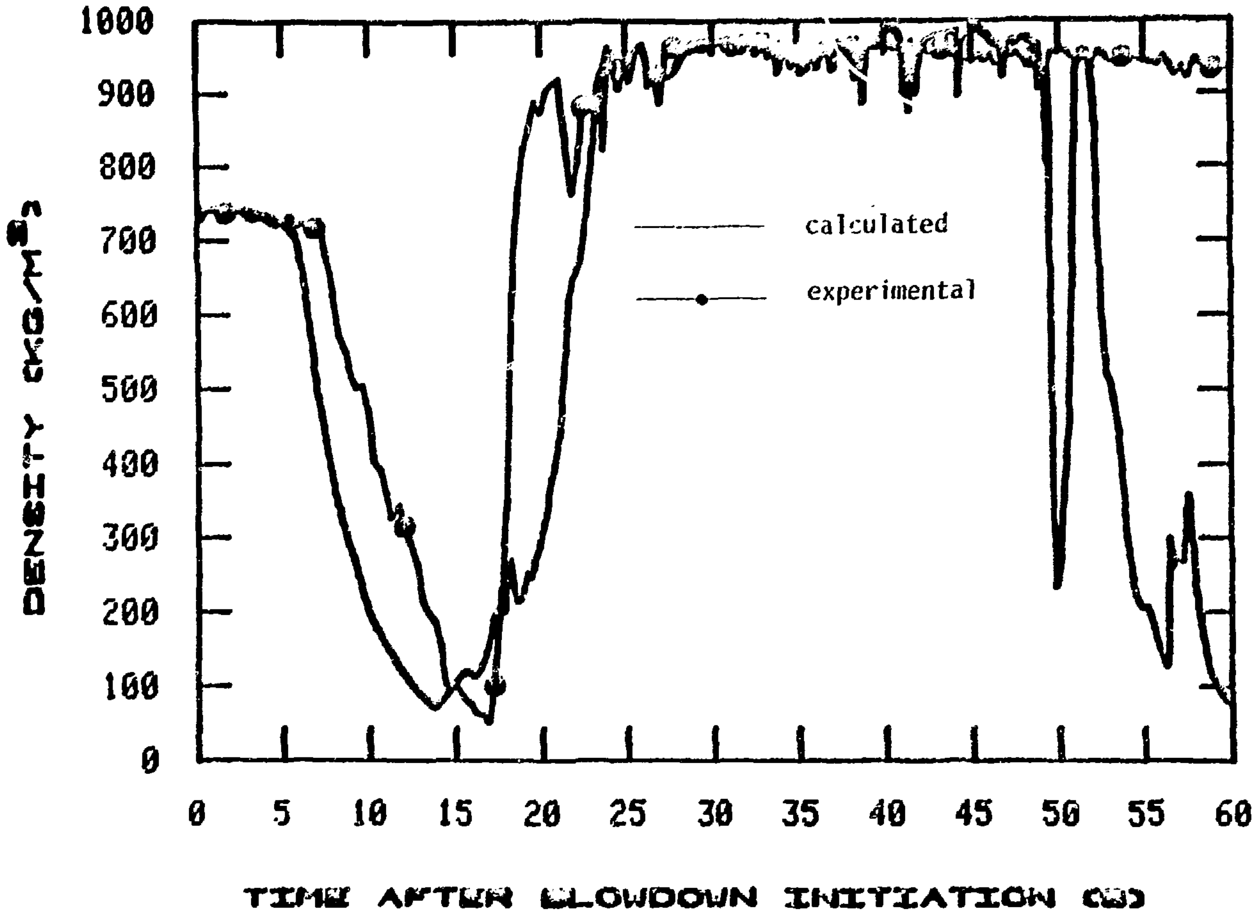

Figure 15 Densities in Broken Loop Cold Leg

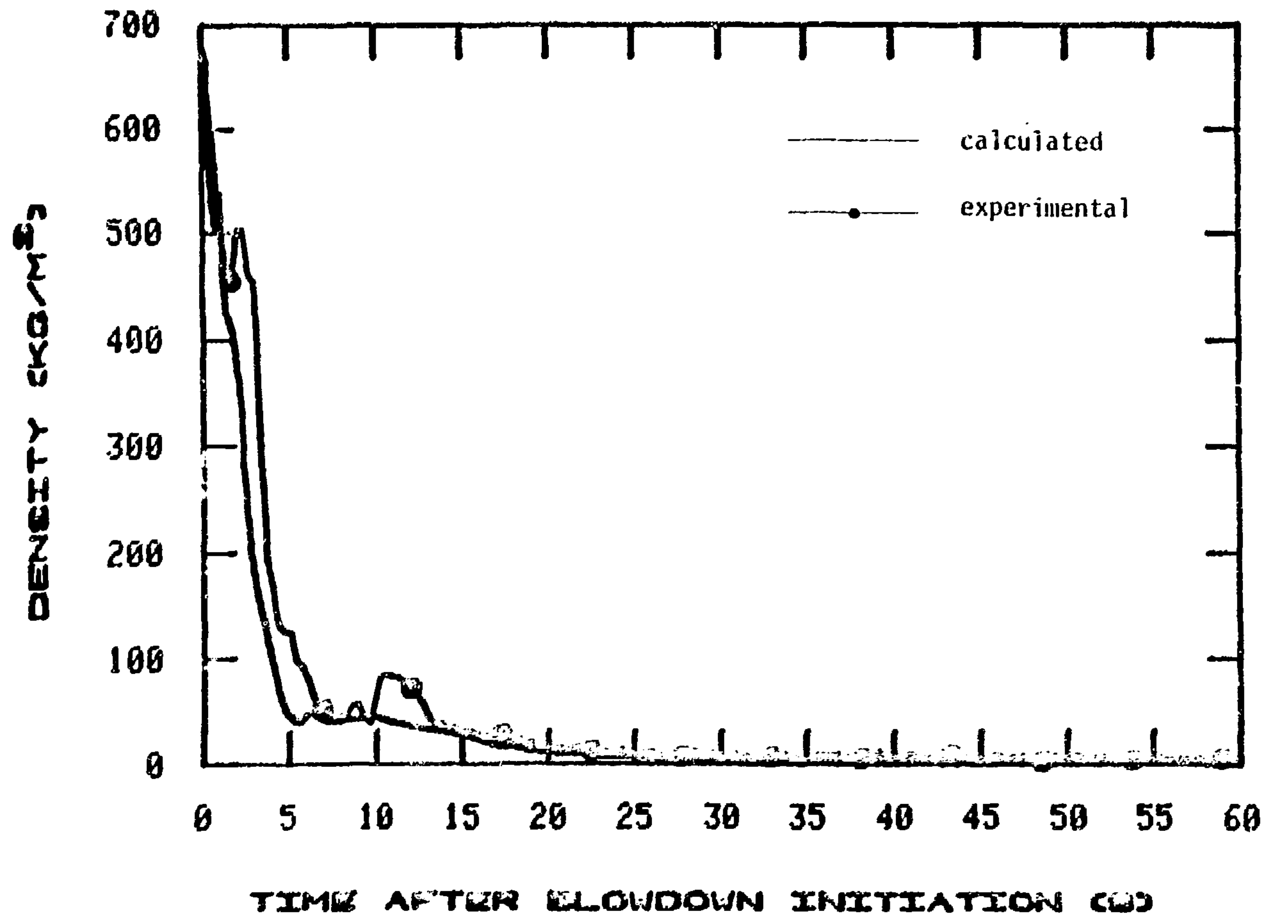

Figure 16 Densities in Intact Loop Hot Leg

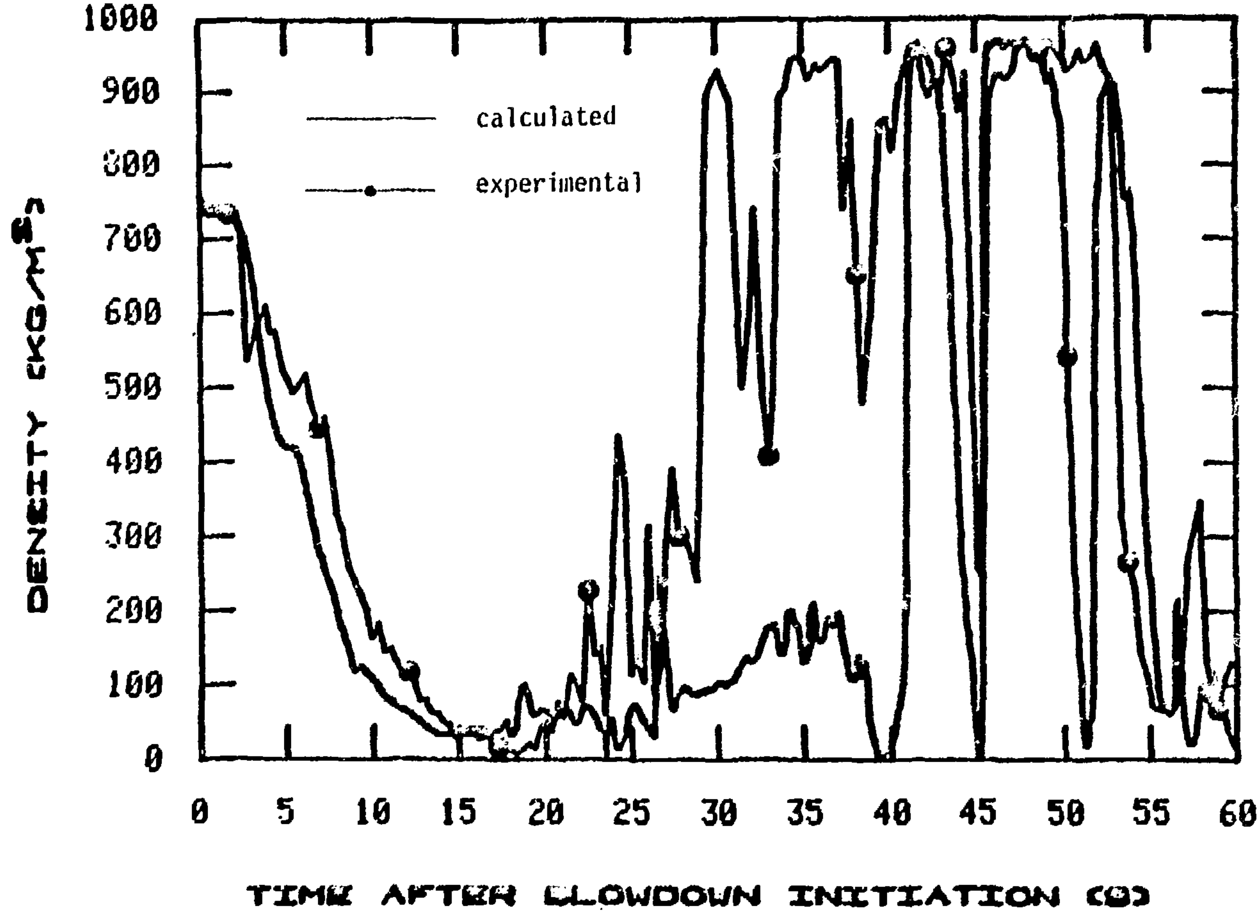

Figure 17 Densities in Intact Loop Cold Leg

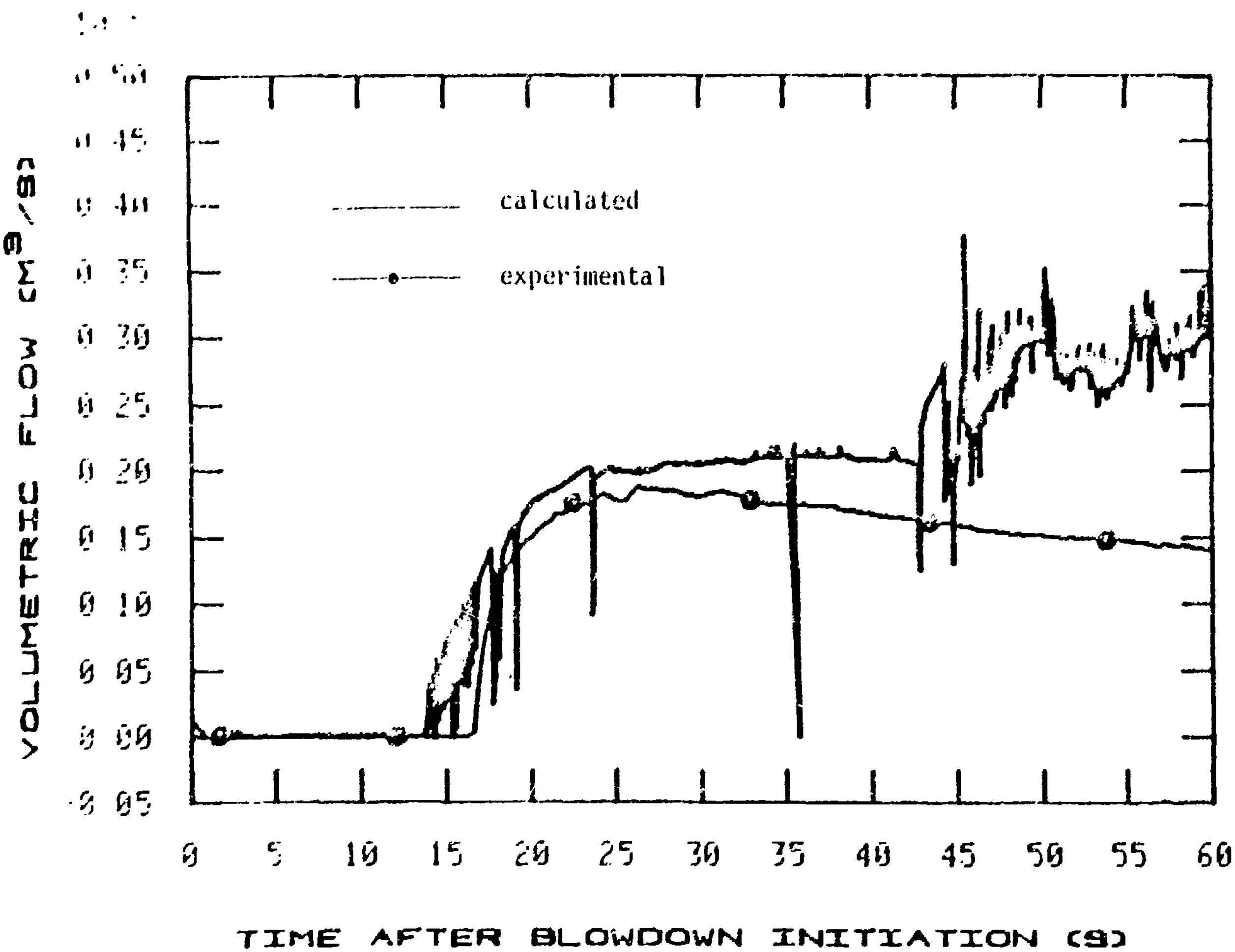

Figure 18 Volumetric Flow in Intact Loop Accumulator

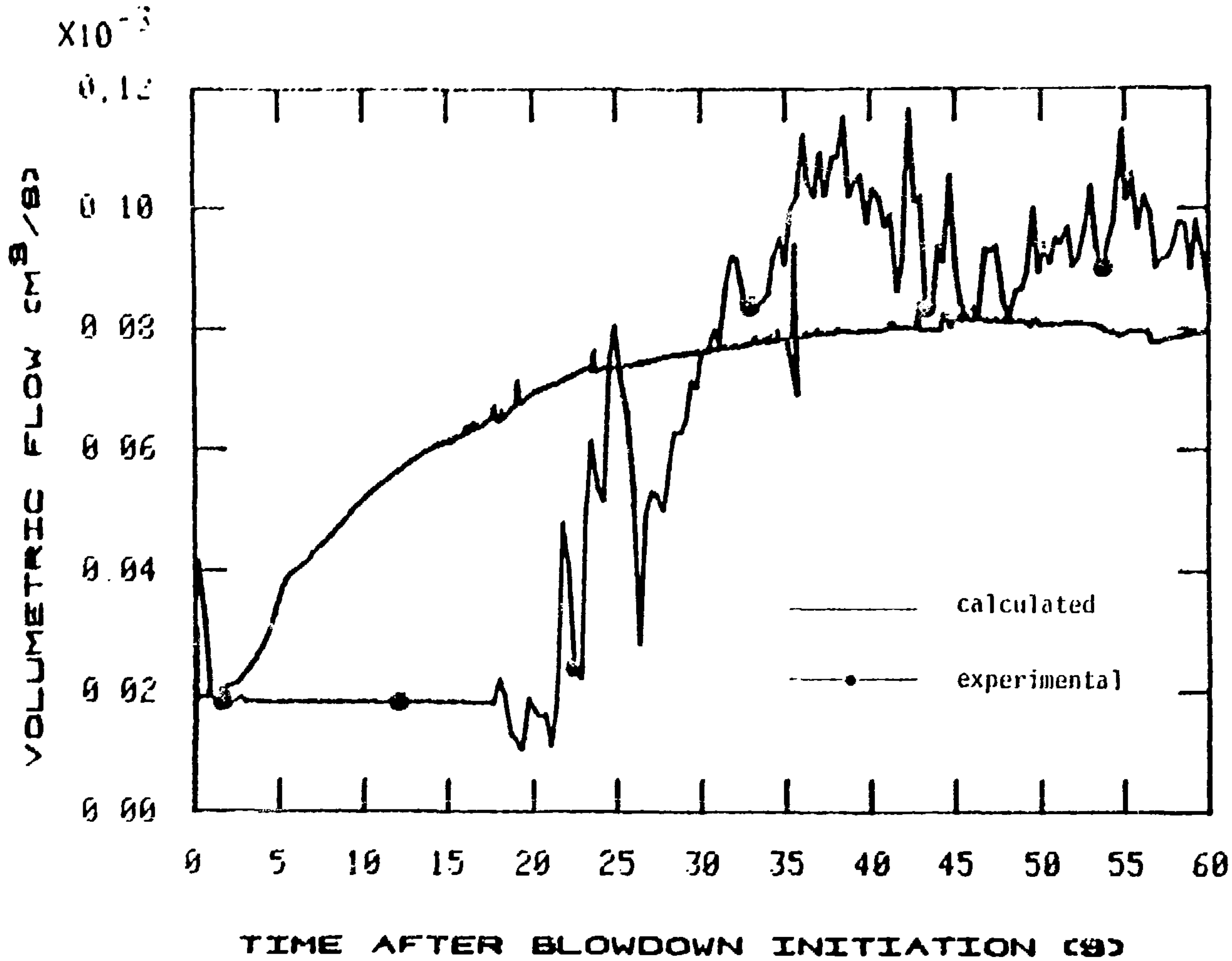

Figure 19 Volumetric Flows in Intact Loop HPIS Pump

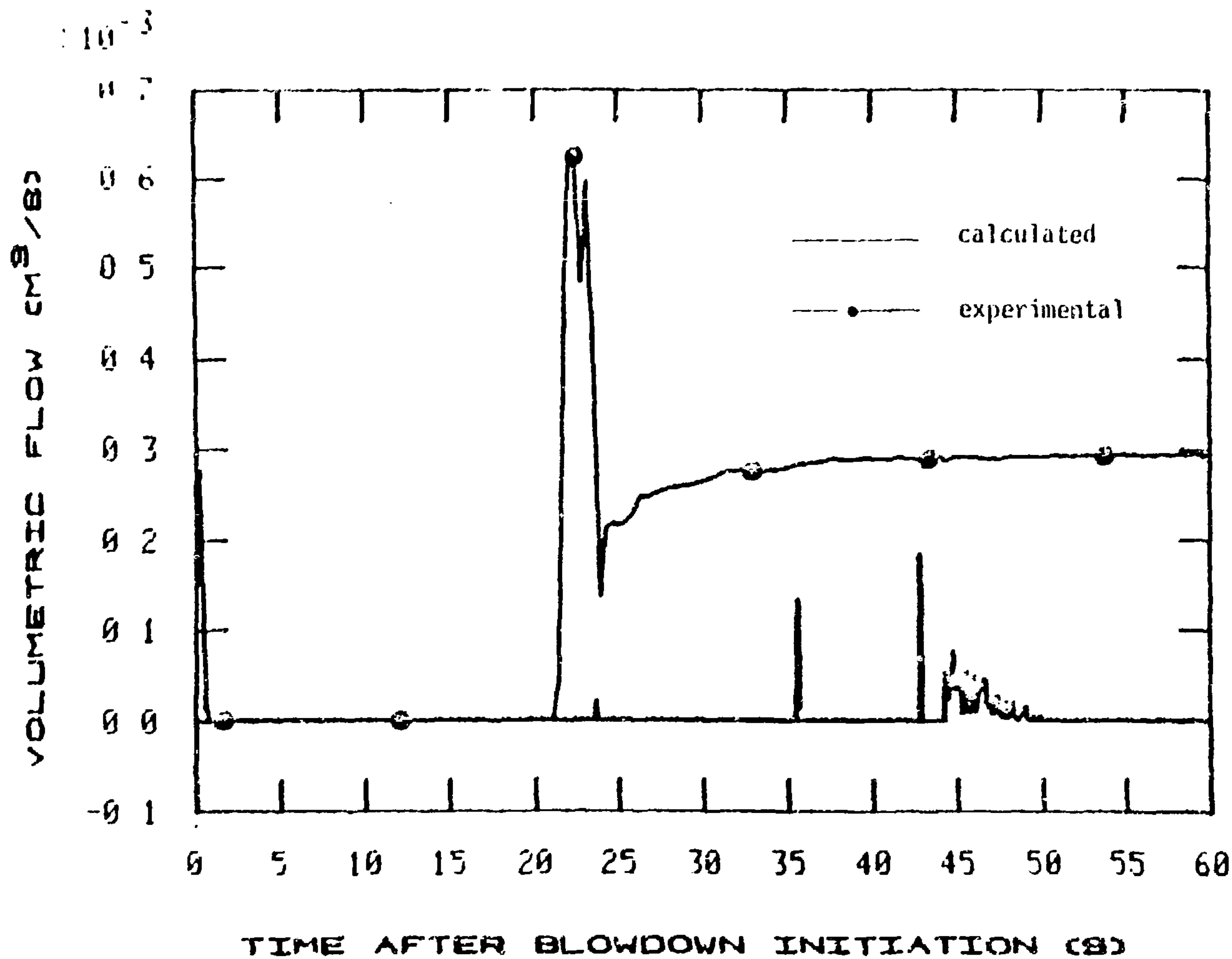

Figure 20 Volumetric Flows in Intact Loop LPIS Pump

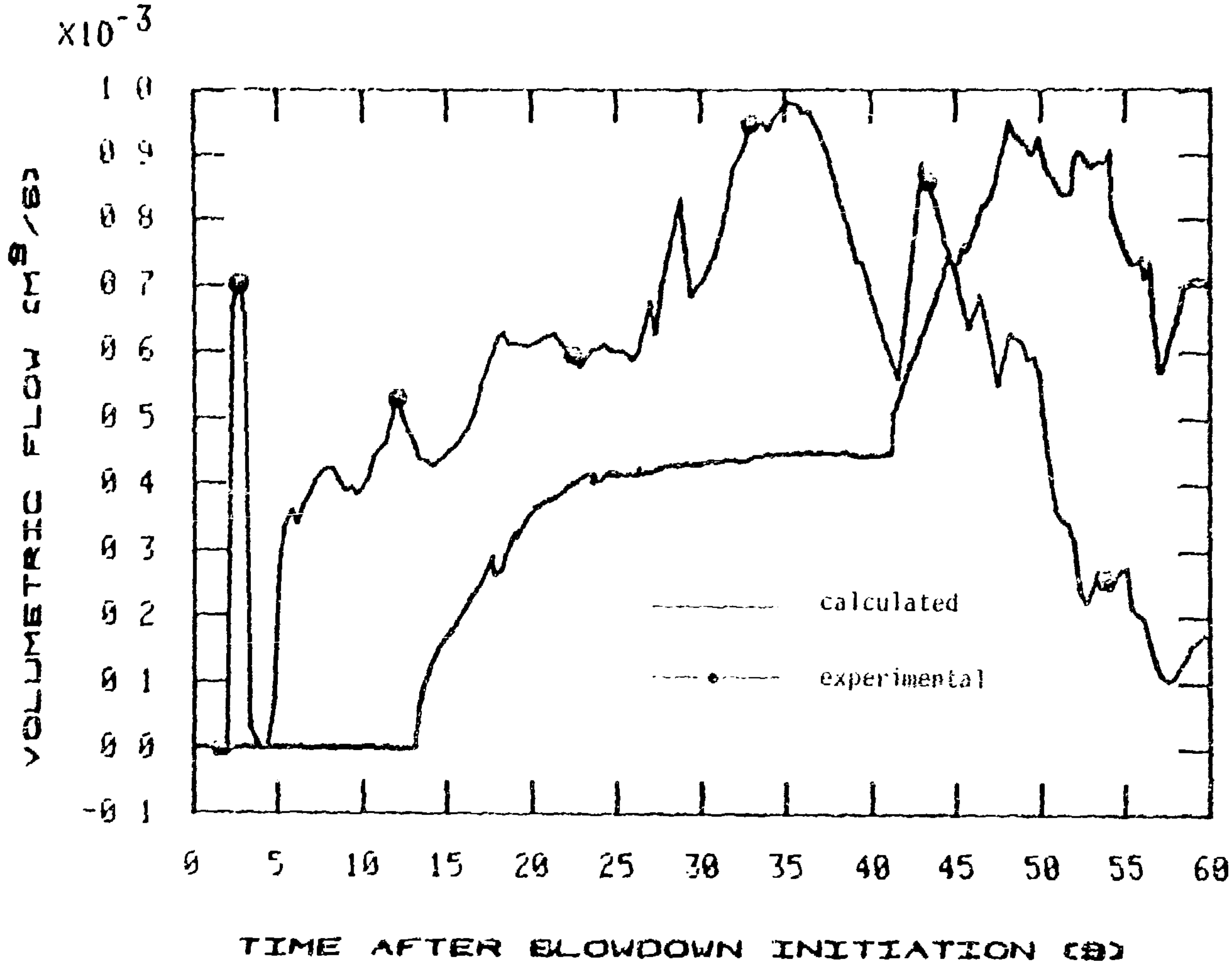

Figure 21 Volumetric Flows in Broken Loop Accumulator

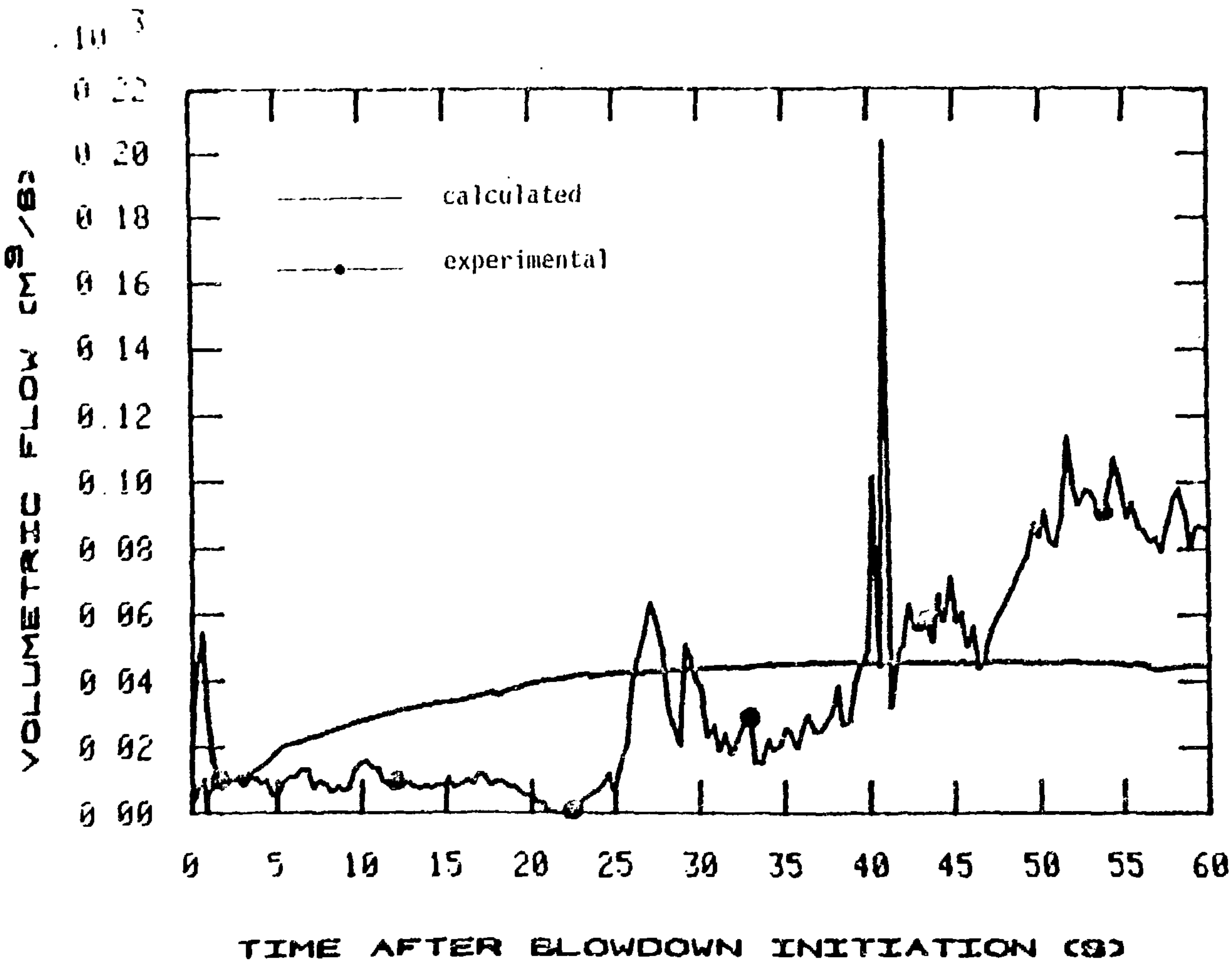

Figure 22 Volumetric Flows in Broken Loop HPIS Pump

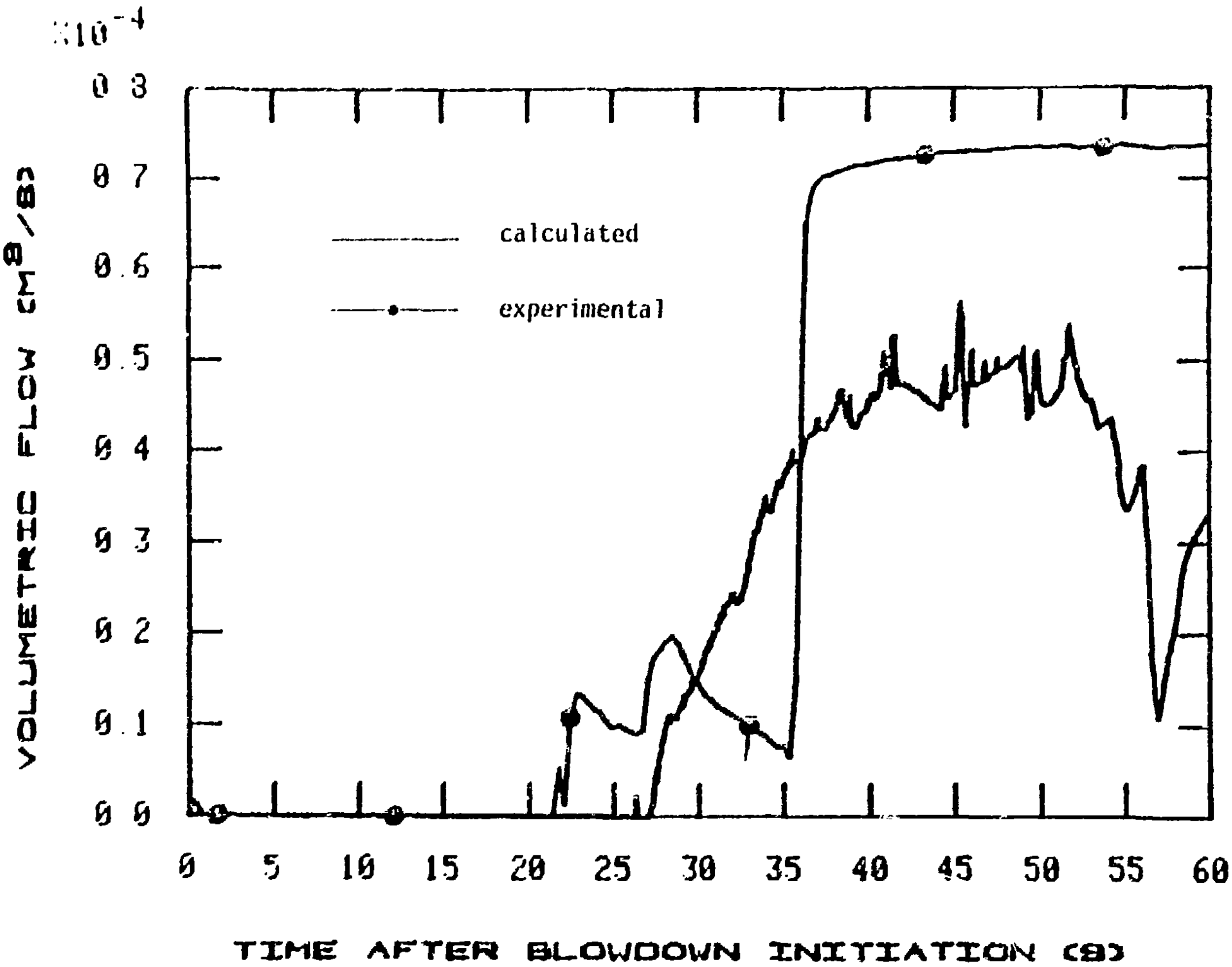

Figure 23 Volumetric Flows in Broken Loop LPIS Pump

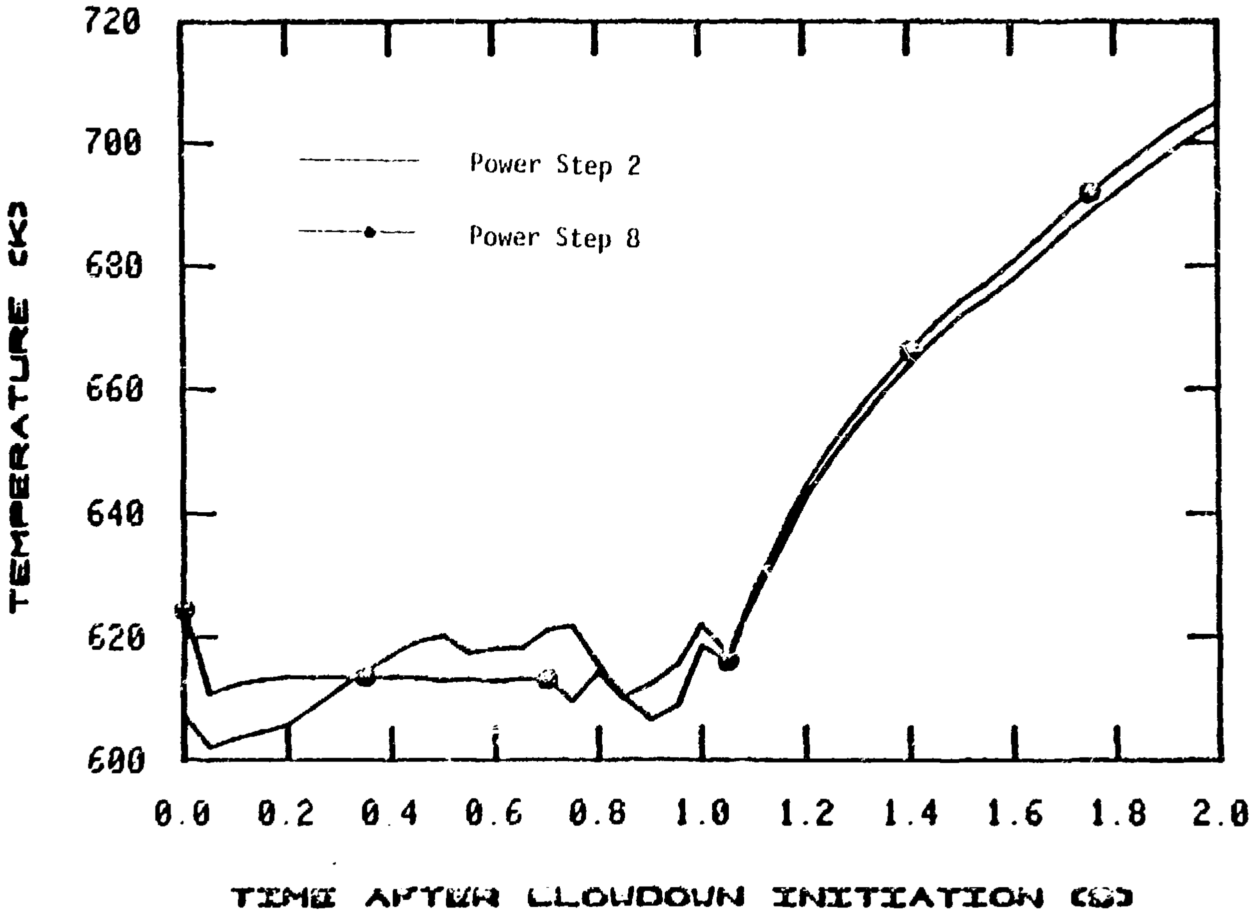

Figure 24 Calculated Cladding Temperatures at Power Steps 2 and 8

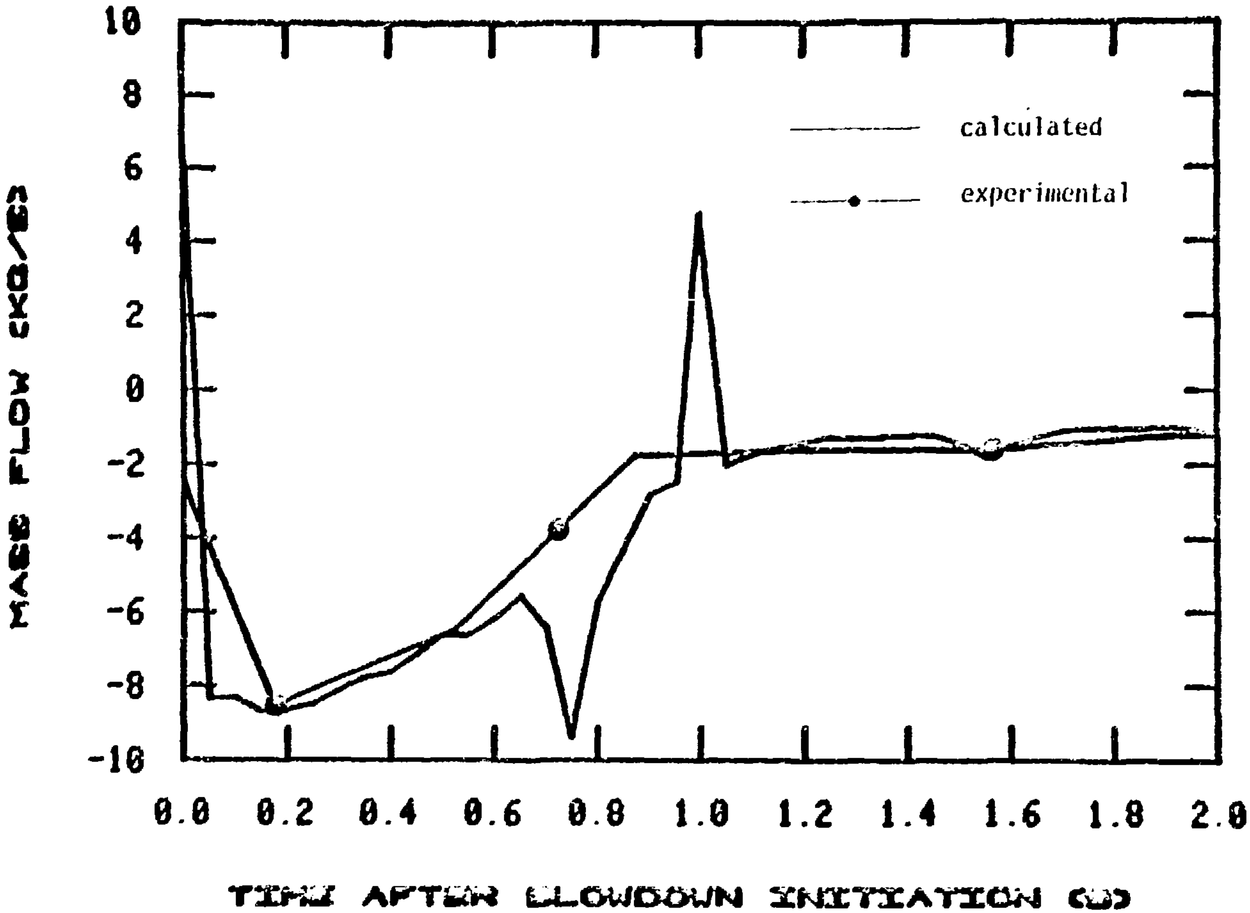

Figure 25 Mass Flows at Core Inlet from 0 to 2s.

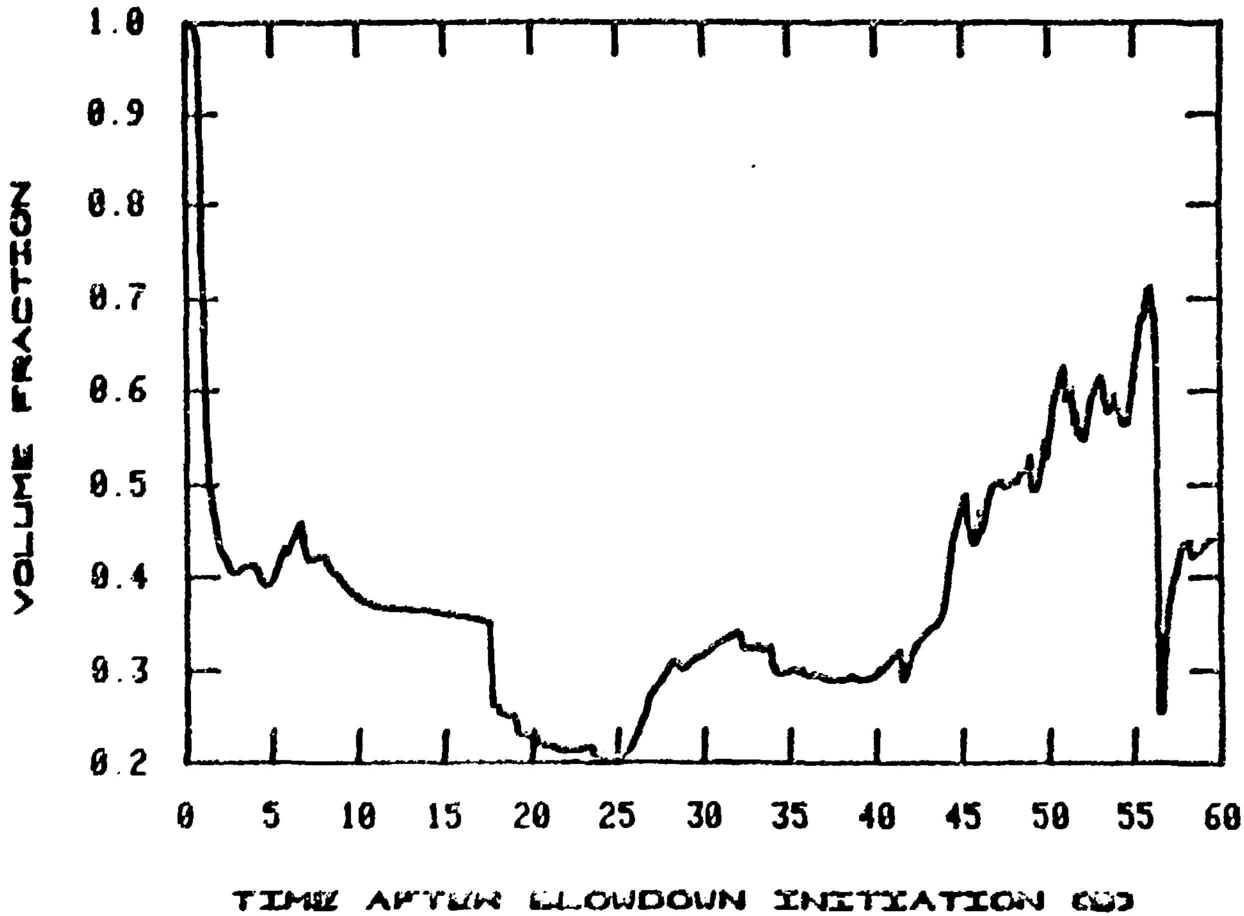

Figure 26 Liquid Volume Fraction in Lower Plenum

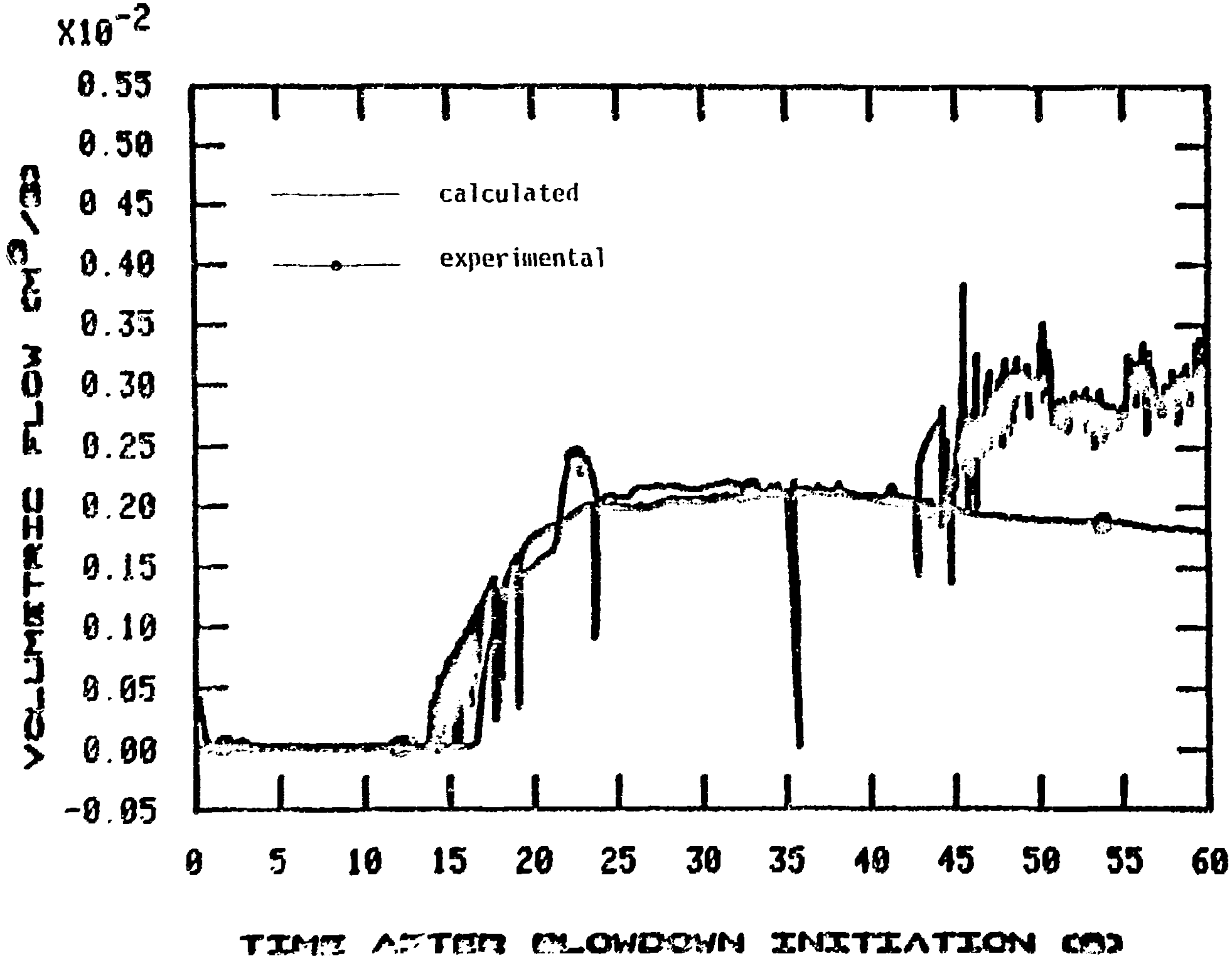

Figure 27 Total Intact Loop ECC Volumetric Flows

Work supported by the U.S. Nuclear Regulatory Commission, Office of RES under DOE Contract No. DE-AC07-76ID01570.